1-1-2015

Evidence Of Distinctive Structural Alterations That Differentiate Adhd Boys With And Without A Comorbid Reading Disability

Dhruman Dilip Goradia
Wayne State University,

EVIDENCE OF DISTINCTIVE STRUCTURAL ALTERATIONS THAT DIFFERENTIATE ADHD BOYS WITH AND WITHOUT A COMORBID READING DISABILITY

by

DHRUMAN DILIP GORDIA

DISSERTATION

Submitted to the Graduate School

of Wayne State University,

Detroit, Michigan

in partial fulfillment of the requirements

for the degree of

DOCTOR OF PHILOSOPHY

2015

MAJOR: TRANSLATIONAL NEUROSCIENCE

Approved By:

_____

Advisor Date

_____

_____

_____

_____

DEDICATION

To my loving family

“Research is to see what everybody else has seen, and to think what nobody else has thought.”

- Albert Szent-Györgyi.

ACKNOWLEDGEMENTS

I am sincerely grateful to my mentor Dr. Jeffrey A. Stanley for providing a nourishing training environment through his wisdom, encouragement and support. He shared his vast knowledge and guided my work with enthusiasm and optimism, which I greatly appreciate. I am also very grateful to Dr. Vaibhav Diwadkar for providing valuable guidance and support throughout my graduate training.

I would like to thank my committee members Dr. Naftali Raz and Dr. Manuel Tancer for helping me with my dissertation and providing valuable feedback, which has enhanced my research abilities. I would also like to specially thank Caroline, Dalal, Rachel, Usha, Olivia, and Ashley for their meticulous job of recruiting, assessing and scanning participants for the study.

I appreciate the financial support provided by Lycaki-Young Funds (State of Michigan), Thomas C. Rumble Fellowship (Wayne State University), and NIMH R01MH065420 (PI: JAS). Without these financial supports my work would not have been possible.

I would like to thank my friends and TNP students for their support and encouragement throughout my program. Finally, I would like to thank my family, particularly my wife Bhavi Shah, for supporting me through all the ups and downs of my life.

TABLE OF CONTENT

LIST OF TABLES

LIST OF FIGURES

CHAPTER 1: Background

1.1 Attention Deficit Hyperactivity Disorder

Attention Deficit Hyperactivity Disorder (ADHD) is one of the most common neurodevelopmental disorders diagnosed in school age children with a general prevalence of approximately 4% to 8% worldwide (American Psychiatric Association, 2000; Faraone, Sergeant, Gillberg, & Biederman, 2003; G. Polanczyk, de Lima, Horta, Biederman, & Rohde, 2007; G. V. Polanczyk, Willcutt, Salum, Kieling, & Rohde, 2014; Thomas, Sanders, Doust, Beller, & Glasziou, 2015; Willcutt, 2012) and tends to have a higher occurrence in boys than girls (Derks, Dolan, Hudziak, Neale, & Boomsma, 2007; Faraone et al., 2003; Willcutt, 2012). Children with ADHD present with impairments in two core symptom domains: inattention and hyperactivity/impulsivity (American Psychiatric Association, 2000). Certain symptoms do diminish with age; however, symptoms can persist into adulthood in as many as 65% of cases (Faraone, Biederman, & Mick, 2006). Additionally, ADHD individuals often exhibit significant deficits in multiple cognitive domains including response inhibition, working memory, sustained attention and motor control (Barkley, 1997; Nigg & Casey, 2005; Sonuga-Barke, 2005). In all, these behavioral impairments and cognitive deficits in children with ADHD lead to poor academic and social outcomes (Currie & Stabile, 2006; Strine et al., 2006) and impact the cost to society in the range of $34 billion to $52 billion annually in the United State (W. E. Pelham, Foster, & Robb, 2007). Despite considerable efforts in the research community, the etiology of ADHD is not fully elucidated.

As noted above, ADHD is symptomatically heterogeneous and is characterized by abnormal levels of inattention, hyperactivity, and impulsivity, either alone or in combination (American Psychiatric Association, 2000). While symptoms of inattention, hyperactivity and impulsivity are often present in all school age children to a certain degree, children with ADHD have greater degree of severity that significantly impact the day-to-day functioning compared to their healthy peers. For the diagnosis of ADHD in children and adolescents, Diagnostic and Statistical Manual version IV Text Revision (DSM-IV-TR) and the recently revised version DSM-V requires the endorsement of 6 out of 9 symptoms related to inattention and/or endorsement of 6 out of 9 symptoms related to hyperactivity/impulsivity (American Psychiatric Association, 2000, 2013). These symptoms must be observed in two settings (e.g. home and school) with some symptoms present prior to 7 years of age (American Psychiatric Association, 2000). The latter criteria has been amended in the revised DSM-V edition (American Psychiatric Association, 2013) to 12 years in order to facilitate diagnosis of ADHD in adults. As in DSM-IV-TR, DSM-V identifies three separate subtypes of ADHD based on symptom presentation. These subtypes are referred to as ADHD-Predominantly Inattentive type, ADHD-Predominantly Hyperactive type and ADHD-Combined type with higher prevalence of the Combined subtype (Faraone, Biederman, Weber, & Russell, 1998; Lahey et al., 1994; Rohde et al., 1999).

While numerous investigations have been conducted to understand the cause of ADHD, the etiology remains poorly understood. Genetic and environmental factors are known to play a role in the development of ADHD. These genetic and environmental factors and its interaction can alter the neurodevelopment processes of the brain.

Evidence does not suggest that neither genetic nor environmental factors can alone cause ADHD (Banerjee, Middleton, & Faraone, 2007). Rather, it is argued that a complex interplay of genetic and environmental factors is responsible for increasing the risk of developing ADHD (Banerjee et al., 2007). Regardless of the underlying etiology, ADHD is considered a neurodevelopmental condition that emerges early in life. In this context, the brain is highly dynamic during the early years of development due to multiple complex processes occurring in a developing brain. Any deviations in these developmental processes can alter the course of brain development resulting in compromised brain morphology. Therefore probing the brain during childhood and adolescence can provide significant insights of neural alterations in ADHD. Numerous investigations have been conducted to identify neural alterations in ADHD; however, there are some inconsistencies in the literature. One of the challenges of in characterizing structural abnormalities associated with ADHD is that ADHD is often complicated with the presence of one or more comorbid conditions. Conditions that commonly co-occur with include conduct disorder/oppositional defiance disorder (CD/ODD), anxiety disorders and depression as well as learning disabilities (Larson, Russ, Kahn, & Halfon, 2011; Spencer, 2006; Spencer, Biederman, & Mick, 2007). Of the different comorbid conditions reading disability (RD) is the most prevalent comorbid condition at about 25% to 45% (Del'Homme, Kim, Loo, Yang, & Smalley, 2007; DuPaul, Gormley, & Laracy, 2013; Willcutt & Pennington, 2000; Yoshimasu et al., 2010). The co-occurrence of RD has been associated with elevated severity of cognitive deficits commonly seen in ADHD (de Jong et al., 2009; Willcutt et al., 2010). However, there are no existing neuroimaging studies that have evaluated the impact of comorbid RD on the

structural abnormalities associated with ADHD. The main aim of this dissertation research was to evaluate the structural correlates of ADHD in the absence (ADHD/-RD) and presence of a comorbid RD (ADHD/+RD).

1.2 Comorbid Reading Disability in ADHD

As noted above, RD is a neurodevelopmental and common condition that co-occur among children with ADHD. RD is one of the learning disabilities that is characterized by persistent problems in reading ability despite adequate cognitive abilities and adequate access to educational resources (American Psychiatric Association, 2000; Germano, Gagliano, & Curatolo, 2010). The prevalence of RD alone ranges from 5% to 10% worldwide (American Psychiatric Association, 2000; Maughan & Carroll, 2006; Pastor & Reuben, 2008; Sexton, Gelhorn, Bell, & Classi, 2012) with higher occurrence in boys than girls (Hawke, Wadsworth, Olson, & DeFries, 2007; Olson, 2002; Rutter et al., 2004; Vogel, 1990). Children with RD present deficits in 3 core symptom domains namely phonology, word recognition and spelling. Additionally, children with ADHD/+RD also present cognitive deficits in working memory, processing speed, attention and response inhibition (Willcutt et al., 2010; Willcutt, Pennington, Olson, Chhabildas, & Hulslander, 2005). Furthermore, these cognitive deficits are shown to be more severe in ADHD/+RD compared to ADHD/-RD or RD alone (Willcutt et al., 2010). Despite the high comorbidity as wells as severe cognitive deficits observed in ADHD/+RD, there are no published studies evaluating the brain morphology differentiating ADHD/+RD from ADHD/-RD.

1.3 Neuroimaging Findings

Advances in the medical imaging technology have allowed researchers to assess the neurobiological correlates of ADHD relative to healthy controls (HC) both cross-sectionally and longitudinally. There is a large body of research providing converging evidence of atypical brain structures in ADHD, in regions that sub-serve the attentional, working memory and cognitive control processes (Arnsten & Rubia, 2012; Valera, Faraone, Murray, & Seidman, 2007). Earlier volumetric studies using magnetic resonance imaging (MRI) have reported significantly reduced total brain volume in children with ADHD; an effect that is most prominent in the prefrontal cortex, striatum, parietal cortex and temporal cortex (Castellanos et al., 2002; Durston et al., 2004; Friedman & Rapoport, 2015; Krain & Castellanos, 2006; Shaw & Rabin, 2009; Valera et al., 2007). One of the largest studies comparing 152 children and adolescents with ADHD and 139 HC has shown cerebral volume to be 3.2% smaller in ADHD group relative to HC (Castellanos et al., 2002). Volumetric studies focusing on specific regional alterations associated with ADHD have found significant volume reductions in the prefrontal cortex (PFC), dorsal anterior cingulate cortex (dACC), parietal cortex (PC), temporal cortex (TC), and Striatum (Durston et al., 2004; Friedman & Rapoport, 2015; Krain & Castellanos, 2006; Shaw & Rabin, 2009; Valera et al., 2007). Furthermore, studies investigating cortical thickness, a measure viewed as being more direct in assessing cortical neural density and cortical development, have also shown thinner cortex in the prefrontal, parietal and temporal cortices (Almeida et al., 2010; Almeida Montes et al., 2013; Batty et al., 2010; Hoekzema et al., 2012; Narr et al., 2009; M. G. Qiu et al., 2011). Additionally, longitudinal studies have also reported

delayed maturation, characterized by the delay in attaining peak cortical thickness, and persistently atypical development of above cortical regions (Shaw et al., 2007; Shaw et al., 2009; Shaw et al., 2006). These regions are the functional core of corticostriatal networks that sub-serve multiple cognitive domains including attention, working memory, cognitive control and motor control, which are often impaired in children with ADHD, as noted above (Barkley, 1997; Nigg & Casey, 2005; Sonuga-Barke, 2005). In addition to cortical and subcortical alterations in gray matter structures, studies investigating white matter volume, integrity and architecture in ADHD compared to HC have found widespread alterations in multiple regions including superior longitudinal fasciculus, corona radiata, inferior longitudinal fasciculus, corpuscallosum and cerebellum (van Ewijk, Heslenfeld, Zwiers, Buitelaar, & Oosterlaan, 2012). Studies investigating white matter alterations using diffusion tensor imaging have found alteration in fractional anisotropy (FA), a non-specific measure of white matter integrity, in the above fiber bundles in children with ADHD (Ashtari et al., 2005; Davenport, Karatekin, White, & Lim, 2010; Kobel et al., 2010; Konrad et al., 2010; Li et al., 2010; Nagel et al., 2011; Peterson et al., 2011; M. G. Qiu et al., 2011; Silk, Vance, Rinehart, Bradshaw, & Cunnington, 2009). However, these finding are inconsistent across studies in terms of directionality of differences with some studies reporting an increase in FA values in the right SLF, right posterior corona radiata (PCR), bilateral ACR, bilateral ILF and left UF of ADHD children (Davenport et al., 2010; Kobel et al., 2010; Konrad et al., 2010; Silk et al., 2009) while other studies reporting a decrease in FA values in the bilateral superior longitudinal fasciculus (SLF), bilateral anterior corona radiata (ACR), bilateral uncinate fasciculus (UF), bilateral cerebellum and right inferior longitudinal

fasciculus (ILF) of ADHD children (Ashtari et al., 2005; Kobel et al., 2010; Konrad et al., 2010; Nagel et al., 2011; M. G. Qiu et al., 2011).

Overall, these neuroimaging observations provide evidence of alteration in the development of corticostriatal networks and thus, support for the hypothesis of altered corticostriatal networks in children with ADHD. However, there is a large variability in the reported findings with regards to regional specificity. This variability can be partly attributed to the heterogeneous samples used by most studies. Studies investigating structural correlates of ADHD use samples that often include common comorbid conditions including a learning disability or specifically RD. The presence of a comorbid RD condition can confound structural findings in ADHD. However, how comorbid RD can impact structural correlates of ADHD children that can differentiate them from ADHD children without comorbid RD has never been published.

1.4 Reading Disability and Implicated Neural Systems

Studies identifying the basis of language development have identified phonological processing and orthographic processing to be the two main processes involved in the acquisition of reading skills. Phonological processing refers to the encoding and decoding of the sound structure of words (i.e. sounding out words) (Cone, Burman, Bitan, Bolger, & Booth, 2008). Orthographic processing refers to the encoding and decoding of the spelling structure of words (i.e. word recognition) (Cone et al., 2008). The phonological processes emerge first, which allows a child to read by sounding out words. As the child masters phonology, orthographic processes start to emerge allowing the child to directly and quickly recognize words. Therefore, the

progression from phonological to orthographic processing is critical in acquiring fluent reading skills. Any deviations in the development of these processes can result in poor reading skills including fluency. Neuropsychological studies have shown that individuals with RD or ADHD/+RD typically have deficits in phonological processing and to a lesser degree in orthographic processing (Willcutt et al., 2010). Neuroimaging studies have identified the left inferior frontal gyrus (Brocca's area), posterior superior temporal gyrus (Wernicke's area), PC and left fusiform gyurs that sub-serve phonological and orthographic processes (Norton, Beach, & Gabrieli, 2015; Sun, Lee, & Kirby, 2010). Furthermore, the left inferior frontal gyrus is shown to be associated with more with phonological processing while the left fusiform gyrus is associated more with orthographic processing (Norton et al., 2015; Sun et al., 2010).

While there is little understanding of the impact of RD on the brain morphology of individuals with ADHD, structural MRI studies in RD have reported significant widespread abnormalities in gray matter regions including the left inferior frontal gyrus (IFG), bilateral superior/middle temporal gyrus, temperoparietooccipital junction, left fusiform gyrus, precunus, and caudate (Norton et al., 2015; Sun et al., 2010). In addition, white matter abnormalities have been reported in the SLF and arcuate fasciculus (AF) (Vandermosten et al., 2012). The SLF and the AF are the major fiber bundles that connect the temporal, parietal and occipital cortex to the frontal cortex and encompass networks that sub-serve reading. On the other hand, ACR is the fiber bundle that connects subcortical structures to the cortical areas and encompass networks that sub-serve executive function including cognitive control.

1.5 Conceptual Framework of ADHD/+RD

The core objective of this dissertation research was to evaluate structural alterations in the brain that may differentiate ADHD/+RD from ADHD/-RD and HC. Based on the neuropsychological findings of shared cognitive deficits that are more pronounced in ADHD/+RD one would predict greater and more widespread morphological alterations in ADHD-related brain areas in ADHD/+RD compared to ADHD/-RD and HC. This includes the striatum, PFC, PC and ACC, which overlaps to a certain extent with that of the implicated areas associated with RD as noted above. Moreover, one would predict additional pathology in regions that are associated with phonological and orthographic processing in ADHD/+RD individuals such as Brocca's area, Wernicke's area and fusiform gyrus. However, most structural neuroimaging studies in ADHD do not address or account for the effects of comorbid RD diagnosis on structural brain alterations. Therefore, it is likely that the results of these studies are confounded by the comorbid RD condition.

The overall aim of the dissertation research is to investigate structural differences in ADHD children and adolescents with and without a comorbid RD diagnosis and HC individuals. In line with the evidence from neuropsychological studies showing relatively greater impairments of multiple domains as well as additional deficits associated with reading impairments in ADHD/+RD relative to ADHD/-RD, it is hypothesize that ADHD/+RD children and adolescents will demonstrate, in general, greater structural neuropathologies compared to ADHD/-RD and HC subjects.

In particular, the aim of the dissertation research is to focus on identifying morphological differences in sub-cortical, cortical and white matter structures in boys

with ADHD/+RD, ADHD/-RD and HC. First, the volume and surface morphology differences in the caudate and putamen between ADHD/+RD, ADHD/-RD and HC was investigated with the hypothesis that ADHD/+RD will show greater degree of morphological alteration relative to ADHD/-RD. The findings differences in surface morphology of the striatum will provide evidence of disruption in the frontostriatal networks that sub-serve cognitive functions and are discussed in Chapter 3. Second, this study will investigate cortical thickness differences between ADHD/+RD, ADHD/-RD and HC with the hypothesis that relative to ADHD/-RD, ADHD/+RD will show greater extent of thinner cortex in regions PFC, PC and ACC that sub-serve cognitive functions as well as Brocca's area, Wernicke's area and fusiform gyrus that sub-serve phonological and orthographic processes. The findings of cortical thickness analysis will provide of distinctive patterns of cortical alterations in ADHD/-RD and ADHD/+RD and are discussed in Chapter 4. Finally, this study will investigate white matter differences using diffusion tensor imaging (DTI) between ADHD/+RD, ADHD/-RD and HC with the hypothesis that relative to ADHD/-RD, ADHD/+RD will show greater degree of abnormality in the FA values in the SLF, AF and ACR. The results of DTI analysis will provide evidence of greater disruption in structural connectivity in the frontostriatal, frontoparietal and reading networks, and are discussed in Chapter 5. In addition, Chapter 2 discusses the general methods used in the dissertation research including study design, data acquisition and pre-processing procedures. Finally, Chapter 6 summarizes the overall findings of the dissertation research.

CHAPTER 2: Study Design, Data Acquisition and Pre-processing

The overall goal of this study was to identify structural correlates that may differentiate between boys with ADHD with and without comorbid RD. To this end, structural alterations are assessed by evaluating group differences in surface deformations of the striatum, cortical thickness and DTI measures of white matter tracks between ADHD/-RD, ADHD/+RD and HC. A structural T_1-weighted MRI scan was used to investigate group differences in striatal (caudate and putamen) shape and cortical thickness. Differences in white matter structure were investigated using diffusion tensor imaging (DTI). This chapter presents an overview of the study design and details the acquisition and pre-processing of imaging data including surface deformation, cortical thickness and DTI metrics of white matter.

2.1 Study Design and Participants

Across all neuroimaging measurements, a cross-sectional study design was used to investigate 37 ADHD diagnosed boys with or without a co-occurring RD diagnosis (ADHD/+RD: n=15 and ages between 6.7 and 14.9 years; ADHD/-RD: n=22 and ages between 6.6 and 14.5 years), and 29 age and IQ matched typically developing healthy control (HC) boys. The ADHD boys were diagnosed using the DSM-IV diagnosis criteria and the rationale to restrict the participants to boys only was due to evidence of distinctive patterns of structural alterations between boys and girls with ADHD as well as higher prevalence of ADHD in boys than girls. Few studies that have investigated structural correlates of ADHD in girls have found significantly reduced

volume of total brain and inferior lobules of the cerebellar vermis compared to healthy control girls (Castellanos et al., 2001). No significant differences in other brain regions including regions that are commonly implicated in boys with ADHD were reported in girls with ADHD (Krain & Castellanos, 2006). These observations suggest that gender can be a significant confounding factor when investigating structural correlation in ADHD. Given the higher prevalence of ADHD among boys, the differences in the developmental profile between boys and girls and the differences in structural correlates of ADHD between genders, the dissertation research focused on boys only. In fact, most neuroimaging studies of ADHD with small sample sizes have included only boys. Participants were recruited as part of the ongoing longitudinal ADHD study (PI: Dr. Jeffrey Stanley; NIMH R01MH065420) from pediatric and adolescent clinics in and around the Detroit (MI) and Windsor (Ontario) area through public advertising. Interested participants were scheduled for a clinical assessment to confirm inclusion/exclusion criteria. Participants who satisfied all inclusion/exclusion criteria, as noted below, underwent a structural MRI/DTI examination. Lastly, prior to entry into the study (clinical assessment and MRI/DTI examination), parents/guardians of the eligible participants provided written informed consent and the participants provided verbal assent. The Wayne State University Institutional Review Board approved the study.

2.1.1 ADHD Assessment

DSM-IV-TR (APA, 2000) criteria were used for the diagnosis of ADHD, which included the following criteria:

1. Have six or more symptoms of inattention that are considered abnormal and are persistent for at least 6 months.
2. Have six or more symptoms of hyperactivity-impulsivity that are considered abnormal and are persistent for at least 6 months.
3. Inattention and/or hyperactivity-impulsivity symptoms being present prior to the age of 7 years.
4. Symptoms present in at least two setting (e.g. home and school).
5. Symptoms should affect social, professional or academic functioning.
6. Symptoms cannot be explained by any other mental or neurological conditions.

Participants diagnosed with ADHD were further classified into ADHD subtypes based on their symptoms. Participants who presented predominantly inattentive symptoms where classified as ADHD-Inattentive type (i.e., criteria #1 above) while participants who presented predominantly hyperactivity-impulsivity symptoms (i.e., criteria #2 above) were classified as ADHD-Hyperactive type. On the other hand, participants who presented both inattentive and hyperactivity-impulsivity symptoms were classified as ADHD-Combine type.

2.1.2 Clinical Assessment

The clinical assessment instruments, which included the Schedule of Affective Disorders and Schizophrenia for School-Aged Children – Present and Lifetime (KSADS-PL), Disruptive Behavior Disorders scale (DBD) and Iowa Conner's hyperactivity/impulsivity scale, were used to diagnose ADHD and other related disorders such as oppositional defiance disorder (ODD) and conduct disorder (CD). The

Wechsler Individual Achievement Test – III (WIAT-III) was used to establish the presence of co-occurring RD. Full scale, verbal and performance IQ was assessed using the Wechsler Abbreviated Scale of Intelligence (WASI). Lastly, demographic information (e.g., DOB, gender, etc.) was also obtained from participants' parents/guardians. The clinical assessments were conducted by two (UR and OM) trained psychologists.

KSADS-PL: KSADS-PL is a semi-structured interview used to diagnose present and lifetime history of psychiatric disorders and provides DSM-IV diagnoses for several psychiatric disorders including ADHD (Kaufman et al., 1997). The interview is administered to both a parent/guardian and the participant.

DBD: DBD is a self-administrated rating scale that is completed by the parents/guardian and teacher (W. E. Pelham, Jr., Gnagy, Greenslade, & Milich, 1992). Based on the answers of 45 questions, the DBD provides an assessment of symptoms related to ADHD, oppositional defiance and conduct behaviors, and establishes any comorbid ODD or CD diagnosis.

Iowa Conner's Hyperactivity/Impulsivity Scale: This is a questionnaire completed by the parents/guardian (37 questions) and teacher (28 questions) that measures symptoms of different dimensions (conduct behaviors, hyperactivity, inattentive-passive, and hyperactivity) in two different settings, the classroom and at home. Published norms are available for children less than 12 years old; unpublished norms are available for adolescents (Loney & Milich, 1982).

Demographics: A demographic form was used to obtain demographic information such as gender, age, socioeconomic status, and education. The parents/guardian of the participants completed a questionnaire.

Wechsler Abbreviated Scale of Intelligence (WASI): The WASI is a paper and pencil test used to measuring verbal and non-verbal intelligence (Wechsler, 1999). The test is composed of 4 subtests: vocabulary, similarities, design and matrix reasoning and results in verbal IQ (VIQ), performance IQ (PIQ) and full scale IQ (FSIQ) scores.

Children's Global Assessment Scale (CGAS): The CGAS score rates the participant's level of impairment in general functioning (Shaffer et al., 1983). The functioning is rated as a score between 1 – 100 regardless of treatment or prognosis.

WIAT-III: WIAT-III is a standardized individual achievement test that provides a measure of reading, written and oral language skills. The scores are normalized for age (Psychological Corporation, 2009).

2.1.3 RD Assessment

All participants completed the WIAT-III assessment. Three normed scores where obtained for each participant: Word Reading Norm, Pseudo-Word Decoding Norm and Spelling Norm. The presence or absence of RD was determined using normalized discrepancy scores from WIAT-III, which are based on WIAT-III achievement scores compared to FSIQ. Participants were considered RD if two out of the three subtest scores eclipsed a discrepancy that is significant at $p = 0.01$ based on the WIAT-III discrepancy score norms (Psychological Corporation, 2009). In case of uncertainty, RD diagnosis was confirmed using consensus from two independent clinical psychologists.

2.1.4 Inclusion and Exclusion Criteria

Inclusion Criteria: For inclusion into the study participants satisfied the following criteria:

1. Must be between ages 6 – 14 years;
2. Must have a full scale IQ of greater than or equal to 80;
3. Must have a CGAS score of greater than or equal to 60.

Exclusion Criteria: The participant were excluded from the study if they satisfied any of the following criteria:

1. ADHD participants were excluded if they also met criteria for a *DSM-IV* Axis-I diagnosis of any psychiatric disorder other than oppositional defiance disorder (ODD), conduct disorder (CD) and/or anxiety disorder;
2. Have a DSM-IV diagnosis of substance abuse in the past 3 months;
3. Current or past history of a significant neurological illness;
4. Have metallic implants or objects in the body that may interfere with MRI/DTI examination.

2.2 MRI/DTI Acquisition

All MRI examinations were performed on a 3 Tesla Siemens Verio whole body system located at the Wayne State University MR Research Facility (MRRF), Harper University Hospital, Detroit, MI. A 12-channel ^{1}H dedicated volume head coil was used for all MRI procedures. The two primary imaging measurements for this study included 7 high-resolution, 3D T_1-weighted volume measurements with different inversion times

(TI) and a DTI measurement with a b-value of 700 s/mm^2 and 55 different gradient directions. The total setup and scan time was approximately 60 min. per subject.

2.2.1 High-Resolution Structural MRI Acquisition

A 3D high-resolution T_1-weighted structural MRI scan was acquired for this study. High-resolution 3D T_1-weighted scans are commonly used for structural neuroimaging studies as it provides high-contrast between gray matter and white matter. The contrast mechanism of T_1-weighted images relies on the differences in the spin-lattice T_1 relaxation time constants of the three main tissue types (gray matter, white matter and CSF). The T_1 relaxation time constant reflects the time required for the longitudinal (z-component) magnetization of the MR signal to return to 63% of its original value after an excitation pulse is applied to rotate the magnetization away from the z-component (Brown & Semelka, 2010).

There are two critical parameters that should be considered for a magnetization-prepared rapid gradient-echo (MPRAGE) sequence: Inversion Time (TI) and Repetition Time (TR). TI refers to the time between the inversion pulse and the first α° RF pulse (Brown & Semelka, 2010). During the TI period, the projection of the magnetization along the longitudinal axis is allowed to recover based on the T_1 time constant to its original value. Since signal from different tissue types will recover at different rates, TI becomes a critical parameter to generate contrast in T_1-weighted images. TI is chosen such that there is large difference in signal from white matter and gray matter tissues while signal from CSF is minimum. TR refers to the time between two successive inversion pulses (Brown & Semelka, 2010). TR period determines how much

longitudinal magnetization has recovered before the successive inversion pulse is applied. Ideally, a long TR should be chosen in order to allow for complete recovery of longitudinal magnetization. However, TR period also determines the total acquisition time of the T_1-weighted image and choosing a long TR parameter will result in unreasonable scan times. Therefore, TR parameter is chosen such that it is long enough to allow maximum recovery of the longitudinal magnetization and short enough to acquire the T_1-weighted image in a reasonable scan time.

At 3T, the estimated T_1 relaxation time ranges between 950 – 1,150 ms for white matter, 1,100 – 1,500 ms for gray matter and >2,000 ms for CSF (De Graaf, 2013). White matter has a shorter T_1 relaxation time and therefore, the magnetization of the white matter signal recovers faster resulting in larger signal or brighter signal intensity on a T_1-weighted image. On the other hand, CSF has a relatively long T_1 relaxation time so the magnetization of the CSF signal recovers slowly resulting in minimal signal and therefore appears dark on a T_1-weighted image. The T_1 relaxation time for gray matter is in-between that of white matter and CSF so they appear gray on a T_1-weighted image.

A 3D magnetization prepared rapid acquisition gradient echo (MPRAGE) sequence was used to acquire T_1-weighted images. MPRAGE sequence is an inversion recovery gradient echo sequence that allows rapid acquisition of 3D T_1-weighted volume. In this sequence, the net longitudinal magnetization is flipped in the -z direction using an inversion (180° RF) pulse. The signal is then allowed to recover for a certain amount of time TI after which a α° RF pulse (flip angle) is applied to flip the recovered magnetization into the xy-plane and signal is collected. The signal from different tissue

types recover at different rates depending on their intrinsic T_1 relaxation properties, which gives rise to the contrast observed in T_1-weighted images.

High-Resolution Structural MRI acquisition protocol: The high resolution 3D T_1-weighted MRI were collected with the following acquisition parameters: TR=2,200ms, Echo Time (TE)= 2.88ms, α= 13º, FOV= 200x256mm^2, 208 axial slices, slice thickness= 0.8 mm, matrix= 250x320, generalized autocalibrating partially parallel acquisition (GRAPPA) = 2 for parallel imaging, and scan-time=6min. To improve signal to noise ratio (SNR) and reduce susceptibility to head motion, seven separate measurements of shorter duration were obtained and averaged offline (Kochunov et al., 2006). Each measurement was collected with a different TI ranging from 766 ms – 808 ms in order to reduce flow artifact.

2.2.2 Diffusion Tensor Imaging Acquisition

Diffusion tensor imaging (DTI) is a powerful MRI technique that provides important information about white matter integrity and architecture by characterizing the directionality and magnitude of the anisotropy of water diffusion within the tissue (Basser, Mattiello, & LeBihan, 1994). The term diffusion refers to the Brownian motion of water molecules and is generally isotropic in free, unrestricted environments. However, in the presence of restriction, as in white matter axonal fibers, the diffusion of water becomes anisotropic (i.e., primarily in the direction of the fibers). The anisotropy of water diffusion can be characterized using a 3x3 diffusion tensor describing the direction and magnitude of water diffusion within the volume of interest. In order to estimate the diffusion tensor, a set of diffusion-weighted MRI images (DWI) must be

collected with six or more different gradient directions such that each gradient direction captures information about the diffusion of water along its direction over the whole brain. The diffusion tensor describes the properties of an ellipsoid in 3D space that represents the degree of anisotropy. Further, by diagonalizing the diffusion tensor, it is decomposed into the three Eigenvalues (λ_1, λ_2 and λ_3) and Eigenvectors (v_1, v_2 and v_3). The three Eigenvalues represent the magnitude of diffusion of water along the three orthogonal axis of the ellipsoid, respectively. The three Eigenvectors represent the direction of the three orthogonal axis of the ellipsoid, respectively. The Eigenvalues can be used to compute the scalar diffusion measurements like fractional anisotropy (FA; Equation 1), axonal diffusivity (DA; Equation 2) or radial diffusivity (DR; Equation 3), which provide insight into the white matter fibers (Le Bihan et al., 2001).

$$FA = \sqrt{\frac{(\lambda_1 - \lambda)^2+(\lambda_2 - \lambda)^2+(\lambda_3 - \lambda)^2}{2\left({\lambda_1}^2 + {\lambda_2}^2 + {\lambda_3}^2\right)}} \qquad (Equation\ 1)$$

$$DA = \lambda_1 \qquad (Equation\ 2)$$

$$DR = \frac{(\lambda_2 + \lambda_3)}{2} \qquad (Equation\ 3)$$

FA quantifies the degree of anisotropy of water diffusion and ranges from 0 to 1 with higher values indicating greater anisotropy (i.e., a probability reflecting an elongated ellipsoid). On the other hand, DA provides information about the magnitude of water diffusion occurring along the axon direction of the ellipsoid while DR provides information about the magnitude of diffusion occurring in the direction perpendicular to the axon direction. Traditionally, FA is one the most commonly reported measures of white matter integrity/degradation (Schneider, Il'yasov, Boltshauser, Hennig, & Martin,

2003; Suzuki, Matsuzawa, Kwee, & Nakada, 2003). Abnormal reductions in FA value may be attributed to myelination loss, fiber density reduction or increase in crossing fibers. However, some authors argue that abnormal increase in FA value may be a consequence of lack of dendritic branching in a region that normally has high levels of branching due to diverse connections and may also infer pathology (Davenport et al., 2010; Silk et al., 2009). Given the uncertainty of interpreting abnormalitiess in FA, addition measures like DA and DR can provide complementary and valuable information about the underlying white matter architecture and/or pathology.

DTI acquisition protocol: The DTI measurement will be collected using a single-shot twice refocused echo planar imaging sequence with the following acquisition parameters: TR= 8,220 ms, TE= 88 ms, FOV= 220x220 mm^2, 51 axial slices, slice thickness= 2 mm, matrix=128x128, b-value= 700 s/mm^2, different gradient directions= 55 with 3 volumes with no diffusion weighting, and scan-time= 8min 23s.

2.3 Pre-Processing of MRI/DTI Data

Pre-processing of all imaging data were done using batch scripts developed in-house on Linux-based system. The pre-processing steps are outlined in detail below.

2.3.1 Pre-processing of High-Resolution Structural MRI data

As noted above, the 3D T_1-weighted high-resolution structural images were acquired in 7 separate volumes. In brief, each volume was pre-processed using an automated pipeline involving NIFTI (a standard neuroimaging file format) conversion, non-uniform intensity correction, de-noising, co-registration and averaging. In detail, the

images were first exported from the scanner in dicom format. The images were converted from Dicom to 3D volumes in standardized NIfTI format using dcm2nii command line tool provided in MRIcron package developed by Chris Rorden (http://www.mccauslandcenter.sc.edu/mricro/mricron/). Following image conversion, each volume segment was visually inspected for motion artifact. Volumes that had excessive motion artifact were discarded from subsequent processing.

The selected volumes were corrected for non-uniform (NU) intensity using NU correction algorithm (Sled, Zijdenbos, & Evans, 1998) optimized for 3T scanner data (Zheng, Chee, & Zagorodnov, 2009) and distributed as part of the FreeSurfer image analysis suite version 5.0.0 (http://www.freesurfer.net). Images collected with high field MRI scanners present NU intensity artifacts in the form of spatially varying intensity within the tissue due to radio frequency (RF) field inhomogeneity, eddy currents and brain anatomy (Sled et al., 1998). This NU intensity artifact can affect quantitative image analysis of MRI data. The NU correction algorithm is an automatic nonparametric method to correct for NU intensity artifact. It has been demonstrated that NU correction method optimized for 3T scanner data can significantly improve segmentation of gray matter and white matter tissues as well as subcortical structures (Zheng et al., 2009).

In addition to NU correction, each segment was de-noised using a spatially adaptive non-local means (SANLM) filter (Manjon, Coupe, Marti-Bonmati, Collins, & Robles, 2010). High-resolution images have an inherently low signal to noise ratio (SNR) because of the small voxel size. While local means filtering approaches are commonly used to improve SNR, these approaches tend to blur structural boundary information. A SANLM filter has been shown to improve SNR while preserving the

structural boundary information. Applying SANLM de-noising filter can improve co-registration accuracy as well as segmentation of brain tissue (Manjon et al., 2010).

After each volume is NU corrected and de-noised, they are averaged using image math tools in FSL (http://fsl.fmrib.ox.ac.uk/fsl/fslwiki/) to obtain an average high-resolution 3D T_1-weighted volume. This average volume was used to analyze surface deformation of the striatum and cortical thickness of the cerebral cortex. The description of the analyses is described in chapter 3 and 4 respectively.

2.3.2 Pre-processing of DTI data

High-resolution DWIs were collected with 55 gradient directions at b=700 s/mm^2 and 3 b=0 s/mm^2. The post-processing of the high-resolution DTI images were done using batch scripts developed in-house using DTIPrep (Liu et al., 2010; Oguz et al., 2014) and FSL-FDT (Behrens et al., 2003) tools on Linux based system. DTI data is susceptible to several kinds of artifacts (e.g., eddy currents, head motion, Venetian blinding, electromagnetic interference, etc) due to inherently low SNR and long scan times (Liu et al., 2010). Therefore, it is necessary to conduct quality check and correct for motion and eddy current artifacts. The quality check and artifact corrections were performed using a fully automated DTIPrep package (http://www.nitrc.org/projects/dtiprep). DTIPrep is a framework for automatic DTI quality control that excludes volumes with high amounts of artifacts and corrects for small head motion and eddy current artifacts (Liu et al., 2010; Oguz et al., 2014). Since motion and eddy current corrections involve rotation of images, appropriate correction of the direction gradient matrix is also necessary (Leemans & Jones, 2009). DTIPrep makes

necessary adjustments to the direction gradient matrix. The quality controlled and artifact corrected data were then de-noised using the SANLM filter to improve the SNR. Following de-noising, the diffusion tensors were estimated using weighted least square method to generate fractional anisotropy (FA), axonal diffusivity (DA) and radial diffusivity (DR) maps. The FA, DA and DR maps were used to assess white matter integrity. The description of the analyses is discussed in chapter 5.

CHAPTER 3: Volume and Shape analysis of the Striatum

3.1 Introduction

Investigations regarding structural correlates of ADHD have consistently implicated cortical and subcortical brain regions including total brain volume, PFC, PC, ACC, cerebellum and striatum (Friedman & Rapoport, 2015; Krain & Castellanos, 2006; Nigg, 2013). Amongst these, structural alterations in the striatum (caudate and putamen) are one of the most replicated finding in ADHD. Structural MRI studies have reported reduced volume in both the caudate (Castellanos et al., 2001; Castellanos et al., 1996; A. Qiu et al., 2009; Semrud-Clikeman, Pliszka, Lancaster, & Liotti, 2006; Tremols et al., 2008) and putamen (A. Qiu et al., 2009; Sobel et al., 2010) of ADHD children compared to healthy controls (HC). On the other hand, little is known of morphological alterations in subcortical areas in ADHD/+RD (Ullman, 2006) including to what extent are observations are similar or dissimilar between ADHD/-RD and ADHD/+RD, given the greater cognitive impairments in ADHD/+RD (Willcutt et al., 2010).

The striatum plays an important role in the processing and integration of information associated with higher order cognitive and motor functions. Anatomically, the striatum receives projections from various cortical areas and these corticostriatal connections are part of the larger cortico-striato-thalamo-cortical networks (Haber & Calzavara, 2009; Haber & Knutson, 2010). Evidence show that the mapping of cortical projections to the striatum is highly organized topographically in a ventral to dorsal and anterior to posterior gradient (Haber & Knutson, 2010). The caudate receives

projections primarily from the prefrontal, parietal and cingulate cortices forming corticostriatal networks that sub-serve executive functions, attention and cognitive control as well as phonological processing (Draganski et al., 2008; Haber & Calzavara, 2009; Haber & Knutson, 2010; Leh, Ptito, Chakravarty, & Strafella, 2007; Lehericy et al., 2004). On the other hand, the putamen receives projections from the motor, premotor and supplementary motor cortices forming corticostriatal networks that sub-serve planning, control and execution of motor functions (Draganski et al., 2008; Haber & Calzavara, 2009; Haber & Knutson, 2010; Leh et al., 2007; Lehericy et al., 2004). Given the nature of the projections and associated cognitive functions, it is not surprising that corticostriatal connections are implicated in children with ADHD as supported by the literature (Bush, 2011).

Given the topographical organization of corticostriatal connections(Draganski et al., 2008; Haber & Knutson, 2010), the interpretation or significance of striatal volume reductions in ADHD as noted above is limited. Assessing morphological deviations along the surface of the caudate and putamen above and beyond the observed volume abnormalities may, however, provide inferences about specific disrupted subareas of the striatum and which corticostriatal projection(s) may be implicated. There are these published studies on surface analysis in ADHD that have shown alterations in surface morphology of the caudate and putamen in ADHD children compared to HC (A. Qiu et al., 2009; Shaw et al., 2014; Sobel et al., 2010). For example, Qiu et al. (2009) found significant clusters of inward deformation in the left medial caudate body, left anterior-lateral caudate head, right medial caudate body and anterior lateral putamen. The study also reports clusters of outward deformation in the left medial caudate head, left medial

caudate tail and medial posterior putamen. Similarly, Sobel et al. (2010) showed significant clusters of inward deformation in the left anterior and dorsomedial caudate head, bilateral ventral caudate body, left anterior and posterior dorsal putamen, left lateral putamen and right anterior-medial putamen. Finally, Shaw et al (2014) showed significant surface area reduction bilaterally extending from head to tail of the caudate, bilateral anterior superior putamen and bilateral posterior inferior putamen. While the results are mostly consistent, there are obvious inconsistencies that may be attributed to differences in sample characteristics. Of the three studies, Qiu et al. (2009) was the only one that explicitly excluded RD as a comorbid condition in their sample of ADHD subjects. Therefore, the results of the other two studies potentially may be confounded by the presence of comorbid RD in the ADHD sample, which is poorly understood with respect to morphological alterations related to RD in ADHD children.

The purpose of this investigation was to identify significant differences in volume and more importantly in the surface morphology of striatal substructures between ADHD boys with and without comorbid RD relative to HC individuals. In line with the evidence from neuropsychological studies showing relatively greater impairments of multiple domains in ADHD/+RD relative to ADHD/-RD as noted in chapter 1, we hypothesize that ADHD/+RD boys will demonstrate greater volume reductions and a greater extent of inward deformation along the caudate and putamen surfaces relative to HC boys in comparison to ADHD/-RD boys relative to HC boys.

3.2 Methods

3.2.1 Sample Characteristics

Group differences in the surface morphology of the striatal structures were assessed in 34 boys with ADHD diagnosis (19 ADHD/-RD and 15 ADHD/+RD) and 24 age-matched HC boys. The diagnosis procedure and inclusion/ exclusion criteria for ADHD and HC are detailed in Chapter 2. Briefly, DSM-IV diagnosis of ADHD was based on clinical neuropsychologists' assessment using the K-SADS, Conner's parent/teacher ratings and DBD parent ratings. The diagnosis of RD was based on WIAT-III assessment and was determined using normalized discrepancy scores from WIAT-III. The ADHD boys consisted of 25 combined type ADHD (11 ADHD/-RD and 14 ADHD/+RD) and 9 inattentive type ADHD (8 ADHD/-RD and 1 ADHD/+RD). Regarding comorbid conditions, the ADHD/-RD subgroup included 7 participants with an oppositional defiance disorder (ODD), whereas the ADHD/+RD included 6 participants with ODD and 1 participant with a separation anxiety disorder. The summary of sample characteristics is tabulated in Table 3.1.

Table 3.1: Sample characteristics

		HC	ADHD/-RD	ADHD/+RD	*Main Term p-value*
Sample Size		25	19	15	
Age (SD)		10.1 (2.2)	11.0 (2.5)	9.6 (2.4)	n.s.
Full Scale IQ (SD)		105 (13)	109 (18)	104 (16)	n.s.
Verbal IQ (SD)		105 (13)	112 (20)	102 (17)	n.s.
Performance IQ (SD)		104 (13)	104 (15)	104 (13)	n.s.
ADHD Subtype	Combined	-	11	14	-
	Innattentive	-	8	1	-
Oppositional Defiane Disorder		-	7	6	-
Conner's Inattention (SD)		-	60 (12)	60 (9)	n.s.
Conner's Hyperactivity (SD)		-	66 (13)	72 (13)	n.s.
Word Reading Norm (SD)		103 (10)	103 (12)	84 (16)[a]	<0.001
Pseudoword Decode Norm (SD)		103 (9)	106 (12)	82 (17)[a]	<0.001
Spelling Norm (SD)		103 (15)	102 (10)	84 (13)[a]	<0.001

[a]Post-hoc results show significant differences compared to both ADHD/-RD and HC (p≤0.001)

3.2.2 Post-Processing and Generating Surface Maps

High-spatial resolution 3D T_1-weighted MRI images were used to delineate the caudate and putamen structures and generate their surface maps. Data acquisition and basic pre-processing steps are discussed in Chapter 2. Briefly, multiple high-spatial resolution 3D T_1-weighted MRI scans collected for each subject were quality checked, NU corrected, de-noised and averaged. These corrected and averaged high-spatial resolution 3D T_1-weighted MRI images were used to generate and analyze surface morphological differences between groups.

The tracing of the caudate and putamen structures were conducted in a two-stage process using FSL tools. As a first approximation, binary masks outlining the caudate and putamen structures separately (i.e., a binary mask for the caudate and putamen structure for each hemisphere) were estimated using the automated FSL-FIRST method (Patenaude, Smith, Kennedy, & Jenkinson, 2011). The outputs for this automated step were then manually corrected by inspecting slice-by-slice in the coronal view and editing pixels on the mask to ensure utmost accuracy in tracing the structural boundaries of the caudate and putamen structures. The guidelines for tracing the caudate and the putamen have been published before (Lacerda et al., 2003; Sanches et al., 2005). For caudate, the anterior boundary was the coronal slice where the caudate first appears; the posterior boundary was the coronal slice where the caudate is no longer visible; the medial boundary is the lateral ventricles; and the lateral boundary was the internal capsule. Special care was taken to exclude the nucleus accumbens. For putamen, the anterior boundary was the coronal slice where the putamen first appears; the posterior boundary was the coronal slice where the putamen is no longer

visible; the medial boundaries are the internal capsule, the nucleus accumbens, and the globus pallidus as we progress from anterior to posterior; and the lateral boundary was the external capsule. Special care was taken to exclude the nucleus accumbens. Two trained raters who were blind to the diagnosis conducted manual editing. The inter-rater reliability was 0.96 for caudate and 0.94 for the putamen.

The manually corrected 3D volume binary masks of the caudate and putamen were then converted to individual 3D surface mesh using the shape analysis toolbox, SPHARM-PDM (http://www.nitrc.org/projects/spharm-pdm). This included transforming the volume masks to spherical harmonics based on shape descriptors and using 2,252 uniformly spaced surface points or vertices to define the surface mesh. The surface meshes were then aligned to a "standard" surface space using the Procrustes alignment approach (Styner et al., 2006) and a randomly selected surface mesh of a control subject as the standard surface space, followed by applying a 3mm FWHM smoothing kernel and averaging the surface meshes of each group in order to generate a study specific template surface mesh. Lastly, deformation surface maps were generated by computing the difference in the signed normal distance between the subject's surface and study specific template at each vertex.

To account for differences in head size, the intracranial volume (ICV) of each subject was also estimated using the output measurement from the Freesurfer's processing pipeline (Buckner et al., 2004). Basically, an atlas based fully automated approach is adopted by freesurfer that relies on the transformation matrix obtained during the normalization of subject's brain to the standard atlas brain. Once the transformation matrix is obtained, the scaling factor parameter is used to estimate the

ICV. Buckner et al. (2004) has demonstrated the reliability and validity of this approach against manual ICV measurement.

3.2.3 Statistical Analysis

Group differences in age, full scale, performance and verbal IQ, reading performance (word reading, pseudoword decoding, and spelling normed scores), and Conner's ADHD symptom scores (inattention and hyperactivity scores) were assessed using one-way analysis of variance (ANOVA; SPSS version 22, IBM Corp.) tests with subject-group (ADHD/-RD, ADHD/+RD and HC) as the main effect term followed by post-hoc analyses of planned contrast comparisons for those group terms reaching significance (i.e., $p > 0.05$). The right and left caudate and putamen volumes were analyzed with age and ICV as covariates using a univariate analysis of covariance (ANCOVA) followed again by post-hoc analyses but with a Bonferroni correction of $p < 0.05$ for significance to control for multiple comparisons.

Statistical analysis of differences between groups in the surface deformation maps of the caudate and putamen structures were conducted using SurfStat (http://www.math.mcgill.ca/keith/surfstat/) and Matlab (The MathWorks Inc.). A multivariate generalized linear model (GLM) was used to assess group differences on the surface deformation maps on a vertex-by-vertex basis and covarying for age and ICV. ICV was included as a covariate to account for differences in head sizes as ICV was significantly correlated with the mean deformation of the caudate and putamen. The false discovery rate (FDR) multiple comparison correction implemented in SurfStat was employed and an FDR corrected p-value of 0.05 was deemed significant. If the

clusters of deformation in the ADHD subgroups were significantly lower than HC, the cluster is considered inward deformation. On the other hand, if the clusters of deformation in the ADHD subgroups were significantly greater than HC, the cluster is considered outward deformation.

3.3 Results

3.3.1 Subject-group characteristics

There were no significant differences between subject groups in age ($F_{2,56}$ = 1.65, p = 0.20), full scale IQ ($F_{2,56}$ = 0.58, p = 0.56), verbal IQ ($F_{2,56}$ = 1.69, p = 0.19) or performance IQ ($F_{2,56}$ = 0.03, p = 0.97). For Conners' composite scores, there was no significant difference between ADHD/-RD and ADHD/+RD in inattention score ($F_{1,32}$ = 0.01, p = 0.92) or hyperactivity score ($F_{1,32}$ = 1.65, p = 0.21). As expected on the WIAT-III scores, there was a significant group effect on Word Reading normed scores ($F_{2,56}$ = 12.34, p < 0.001), Pseudoword Decoding normed scores ($F_{2,56}$ = 18.32, p < 0.001), and Spelling normed scores ($F_{2,56}$ = 10.69, p < 0.001) with post hoc analyses showing significantly worst performance in the ADHD/+RD group compared to both ADHD/-RD and HC on these three reading scores ($p \leq 0.001$) and no significant differences between ADHD/-RD and HC. Table 3.1 includes a summary of the results.

3.3.2 Volume Measurements

ICV: There were no significant differences between subject groups in ICV ($F_{2,54}$ = 1.22, p = 0.30) after controlling for age.

Caudate: Univariate analyses showed a significant group effect on caudate volume bilaterally (Right: $F_{2,54}$ = 6.36, p = 0.003; Left: $F_{2,54}$ = 8.64, p = 0.001). Planned

contrast comparisons showed significantly reduced left (p = 0.012), but not right (p = 0.29) caudate volume in ADHD/-RD boys relative to HC boys, and significantly reduced caudate volume bilaterally (Right: p = 0.002; Left: p = 0.001) in ADHD/+RD boys relative to HC boys (Figure 3.1). There was no significant difference in caudate volume between ADHD/-RD and ADHD/+RD (Right: p = 0.21; Left: p = 1.00).

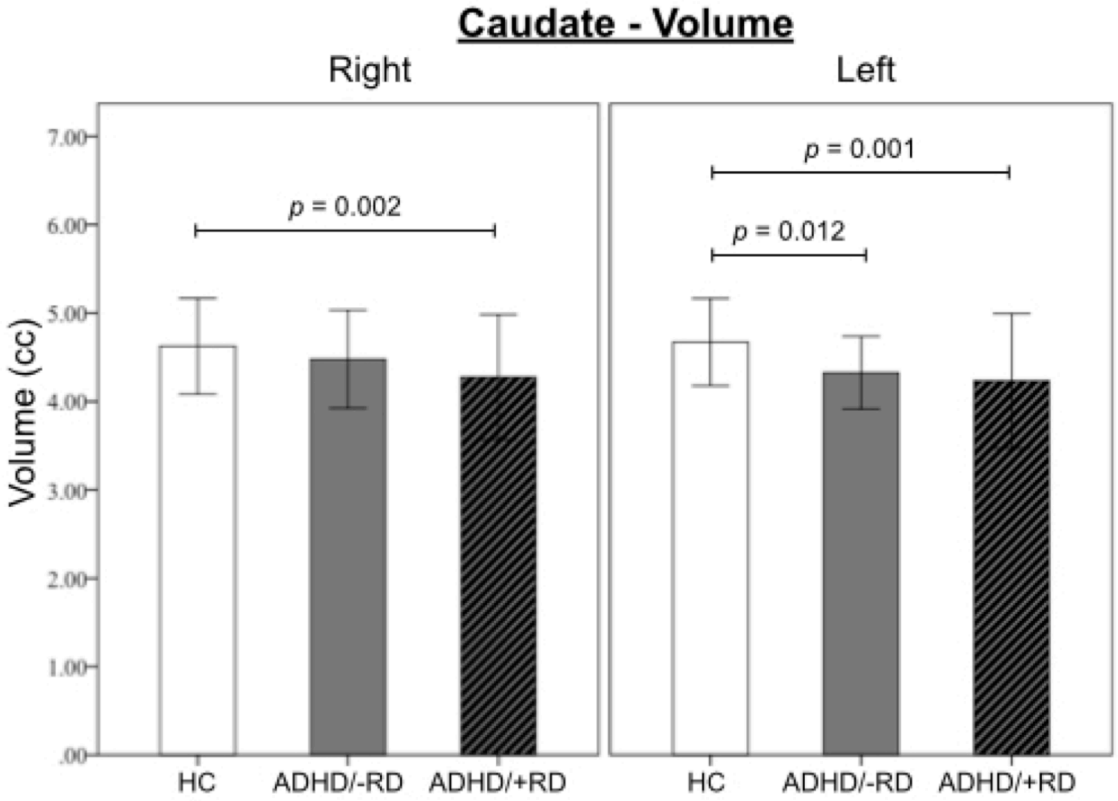

Figure 3.1: Results of group comparison of caudate volumes. With the group term being significant, post hoc analyses show significant volume reduction bilaterally in the caudate of ADHD/+RD boys and on the left side of ADHD/-RD boys, both compared to HC.

Putamen: Univariate analyses showed a significant group effect on the putamen volume bilaterally (Right: $F_{2,54}$ = 5.08, p = 0.01; Left: $F_{2,54}$ = 4.09, p = 0.022). Planned contrast comparisons showed significantly reduced putamen volumes bilaterally in ADHD/-RD boys compared to HC boys (Right: p = 0.01; Left: p = 0.023), and no significant difference in putamen volumes between ADHD/+RD and HC groups (Right: p = 1.00; Left: p = 1.00) (Figure 3.2). There were no significant differences in caudate volume between ADHD/-RD and ADHD/+RD (Right: p = 0.09; Left: p = 0.14).

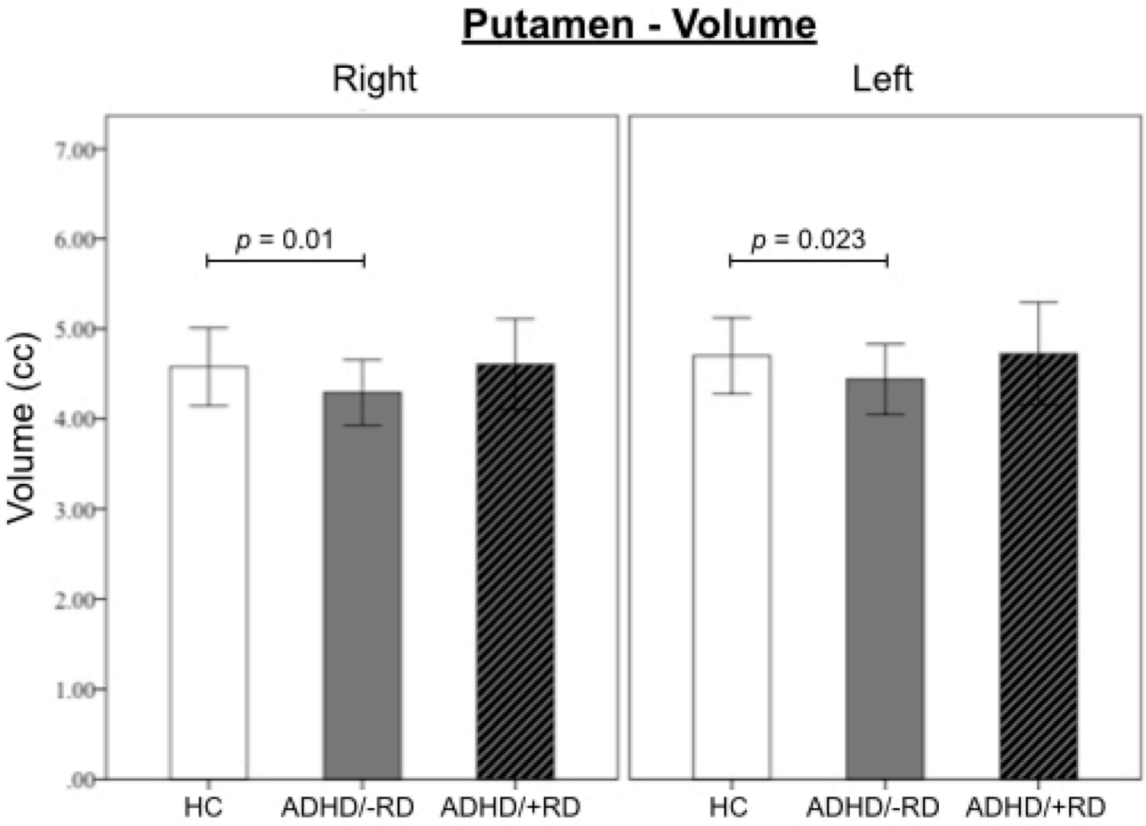

Figure 3.2: Results of group comparison of putamen volumes. With the group term being significant, post hoc analyses show significant volume reduction bilaterally in the putamen of ADHD/-RD boys compared to HC.

3.3.3 Surface Deformation Measurements

Caudate: GLM analysis comparing deformation at each vertex along the surface of the caudate structure of ADHD subgroups to HC showed multiple significant clusters of vertices reflecting inward deformation throughout the caudate structure (Figures 3.3 & 3.4; Table 3.2). Relative to HC, ADHD/-RD showed significant, FDR-corrected clusters of vertices reflecting inward deformation in the medial caudate surface in the left anterior and middle-posterior areas (Figure 3.3; Table 3.2). In contrast, comparison of ADHD/+RD to HC showed widespread significant, FDR-corrected clusters of vertices reflecting inward deformation in the medial caudate surface in the right anterior, right middle-posterior, and left anterior-posterior areas (Figure 3.4; Table 3.2). There were no differences in surface deformations between ADHD/-RD and ADHD/+RD after FDR correction.

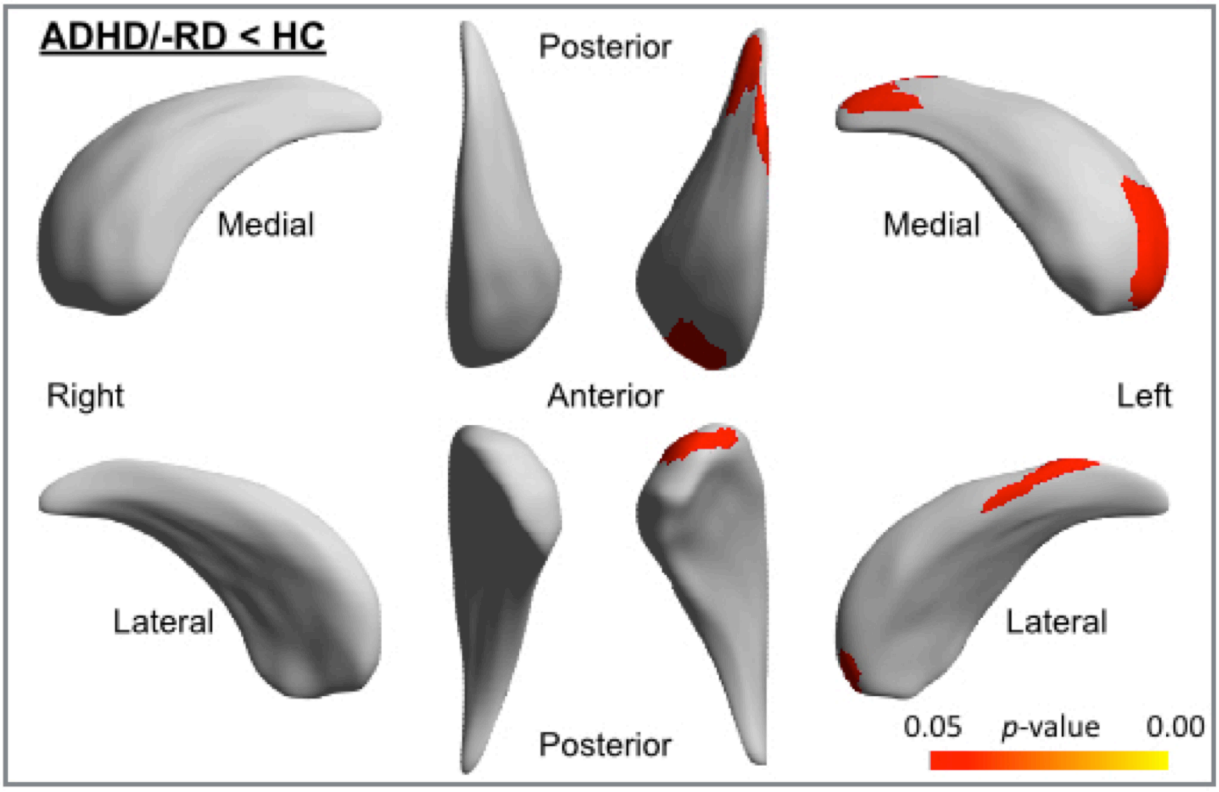

Figure 3.3: Results of surface deformation comparison of the caudate between ADHD/-RD and HC. Compared to HC, results show significant clusters of inward deformations in the left medial/dorsal portion of the anterior and bilateral posterior surfaces of ADHD/-RD boys.

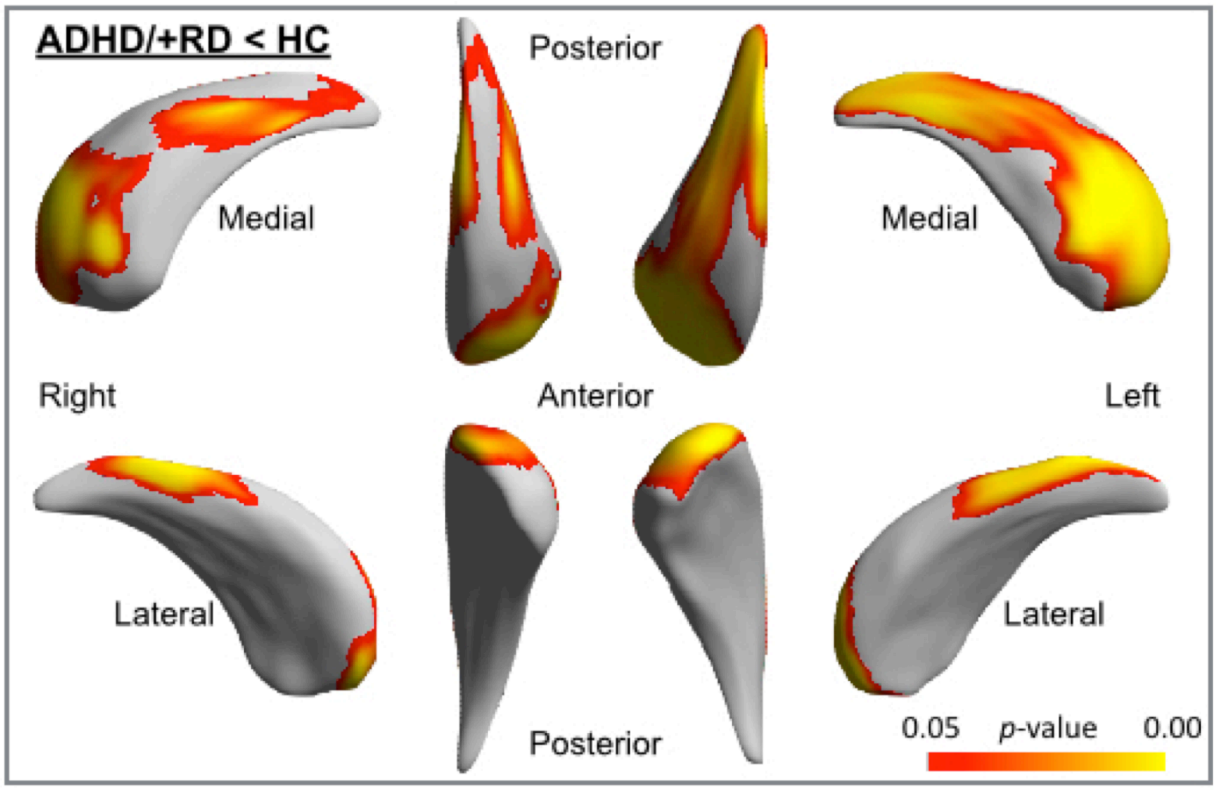

Figure 3.4: Results of surface deformation comparison of the caudate between ADHD/+RD and HC. Compared to HC, results show significant clusters of inward deformations in the left medial/dorsal portion of the caudate surface from the anterior to posterior edges and the right medial/dorsal portion of the anterior and posterior surfaces of ADHD/+RD.

Table 3.2: Results of surface deformation analysis of the striatum in boys with ADHD with and without RD relative to HC.

Comparison	Region Of Interest	Location	Side	Cluster Size (Vertices)	Surface Area (mm^2)	t	FDR *p*
ADHD/-RD < HC	Caudate	Medial Anterior	Left	150	180.22	4.09	0.021
		Medial Middle-Posterior	Left	82	102.68	2.80	0.039
	Putamen	Medial to Lateral Anterior	Right	419	349.98	4.56	<0.001
		Dorsal Lateral Posterior	Right	249	222.31	5.88	<0.001
		Medial to Lateral Anterior	Left	448	330.85	5.96	<0.001
		Dorsal Lateral Posterior	Left	265	208.76	4.59	<0.001
ADHD/+RD < HC	Caudate	Medial Anterior	Right	395	421.86	4.56	0.003
		Medial Middle-Posterior	Right	265	310.84	5.01	0.003
		Medial Anterior-Posterior	Left	934	971.57	4.56	0.003

Putamen: GLM analysis comparing surface deformations between ADHD subgroups and HC showed multiple clusters reflecting inward deformation along the putamen surfaces (Figure 3.5; Table 3.2). Specifically and relative to HC, ADHD/-RD showed significant, FDR-corrected clusters of vertices reflecting inward deformation bilaterally in the medial-lateral anterior and dorsal-lateral posterior surfaces (Figure 3.5; Table 3.2). In contrast, there were no significant differences in surface deformations between ADHD/+RD and HC after FDR correction.

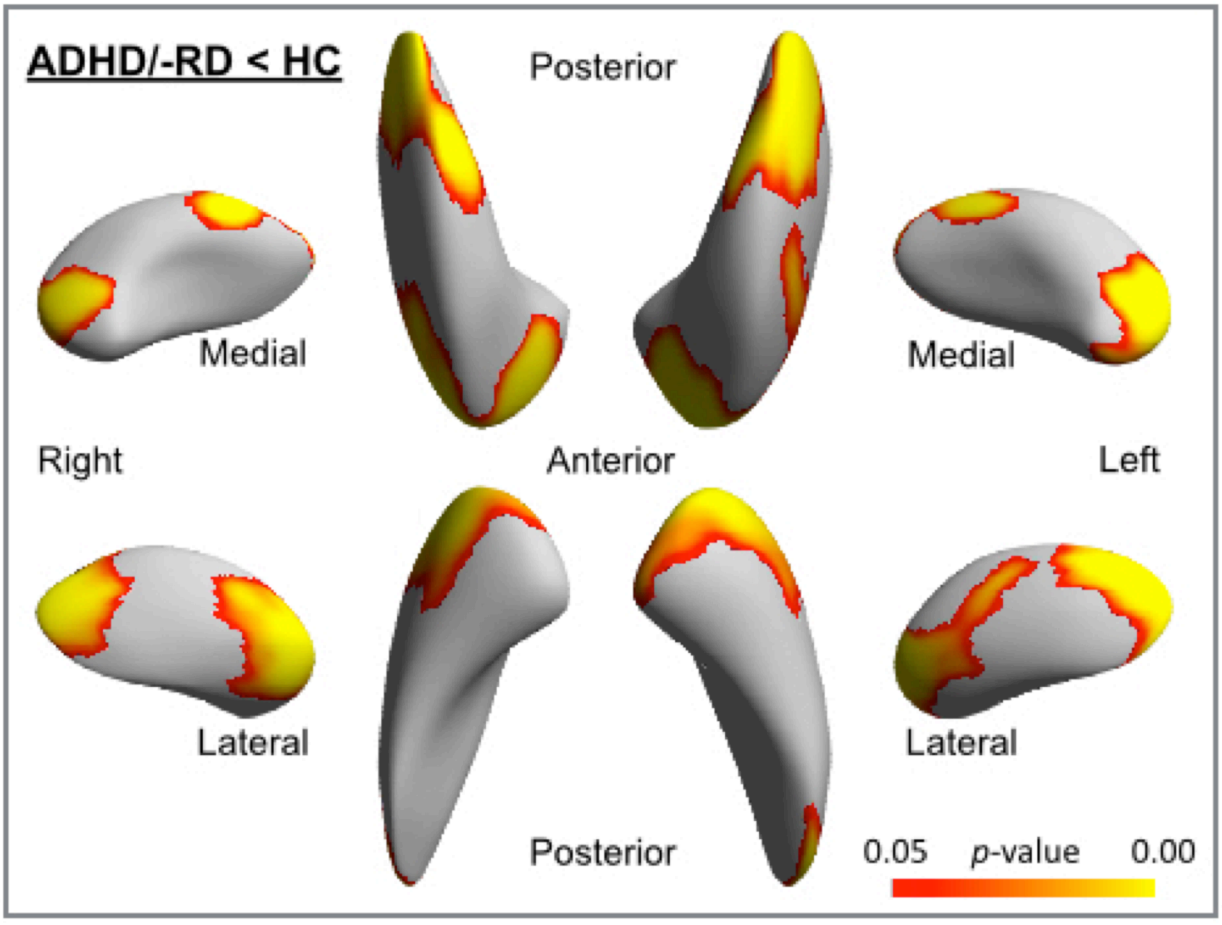

Figure 3.5: Results of surface deformation comparison of the putamen between ADHD/-RD and HC. Compared to HC, results show significant clusters of inward deformations in the anterior and posterior surface bilaterally in ADHD/-RD. *Note.* ADHD/+RD did not show any significant clusters of deformation.

3.4 Discussion

This study investigated differences in volume and surface morphology of the striatal substructures between boys with ADHD with and without comorbid RD relative to HC boys. In line with numerous other reports, we found reduced caudate volume in ADHD subgroups relative to HC. Specifically, the results showed caudate volume deficits only on the left side of ADHD/-RD compared to HC, but the effect was bilateral and to a greater degree in ADHD/+RD compared to HC (Figure 3.1). In contrast, bilateral putamen volume deficits were specific to ADHD/-RD and not present in ADHD/+RD both compared to HC (Figure 3.2). Subsequent investigations identifying where along the structural surface these volume deficits exist showed significant clusters reflecting inward deformation along the left anterior and middle/posterior surface of the caudate in ADHD/-RD compared to HC (Figure 3.3). As hypothesized, there were greater and more widespread significant clusters reflecting inward deformation in the caudate in ADHD/+RD compared to HC (Figure 3.4). In contrast, surface analysis of the putamen show significant clusters reflecting inward deformations along the anterior and posterior surfaces only in ADHD/-RD relative to HC (Figure 3.5). These are important findings showing, for the first time, specific and unique alterations differentiating ADHD/+RD from ADHD/-RD and HC.

Boys with ADHD/-RD showed significant volume reduction in the left caudate and bilateral putamen relative to HC. Consistent with our volume finding, surface based analysis in ADHD/-RD boys showed significant clusters of vertices reflecting inward deformation along the left caudate and bilateral putamen surfaces. It has been suggested that the volume reduction in the striatum may disrupt corticostriatal sub-

networks (A. Qiu et al., 2009; Sobel et al., 2010) resulting in impairment of functions that are sub-served by these corticostriatal networks. In the caudate, significant inward deformations were seen in the left anterior and posterior surface. In the putamen, significant inward deformations were seen in the bilateral anterior and posterior surface, and in the left middle surface. These results are consistent with previous finding of inward deformation in the caudate and putamen in children with ADHD compared to HC (A. Qiu et al., 2009; Shaw et al., 2014; Sobel et al., 2010). Given the highly organized nature of the striatum (Haber & Calzavara, 2009; Haber & Knutson, 2010), these clusters of inward deformation may implicate the prefrontal cortex, specifically the ventral areas, and the cingulate cortex. This is supported by evidence of morphometric alterations observed in children with ADHD including reduced volume and thinner cortex of the prefrontal and cingulate cortex (Friedman & Rapoport, 2015; Krain & Castellanos, 2006; Nigg, 2013). Structural alterations in the cortex and striatum may underpin the impaired executive function, attention and cognitive control observed in ADHD.

By contrast, boys with ADHD/+RD showed significant bilateral volume reduction in the caudate only, and not the putamen, relative to HC. ADHD/+RD also showed a greater volume reduction when compared to HC. These results suggest that boys with ADHD/+RD may present with a greater volume reduction than ADHD/-RD in the caudate. Similar to the pattern of decreased volume, boys with ADHD/+RD showed significant inward deformations only in the caudate bilaterally relative to HC. The left caudate showed inward deformation that extended from the anterior surface to the posterior surfaces. Both ADHD/-RD and ADHD/+RD show inward deformation in the left anterior and posterior caudate surface with ADHD/+RD boys showing greater spatial

extent of inward deformation than ADHD/-RD (Figures 3.3 & 3.4). Furthermore, ADHD/+RD group shows additional inward deformations in the right anterior and bilateral middle caudate surface (Figure 3.4). These results suggest that ADHD/+RD boys demonstrate excessive morphological alteration in the caudate in contrast to ADHD/-RD boys. The observation of excessive and additional inward deformation along with greater volume reduction in the caudate in ADHD/+RD group may implicate greater and more widespread morphological alterations in the prefrontal and cingulate cortices. The excessive morphological alterations in the caudate and possibly in the prefrontal and cingulate cortices of boys with ADHD/+RD may underpin the greater impairment in the attention and cognitive domains observed in neuropsychological studies (Willcutt et al., 2010).

Regarding the putamen, only ADHD/-RD boys show significant volume reduction and inward deformation bilaterally relative to HC. ADHD/+RD boys did not show any significant deformations, after correcting for multiple comparisons. However, uncorrected map shows significant clusters of inward deformation in areas that are similar to those seen when ADHD/-RD was compared with HC suggesting that the sample may not have adequate statistical power, particularly since the ADHD/-RD sample has only 15 subjects. Compressed areas in the uncorrected map include the anterior and posterior putamen surface bilaterally, and may be detectable after multiple comparison correction for ADHD/+RD with larger sample size. This suggests a similar morphological alteration in the putamen in both ADHD/+RD and ADHD/-RD boys, which may be associated to the hyperactive symptoms displayed by both groups.

Furthermore, it also suggests that putamen morphology in ADHD may not be associated with the presence of co-occurring RD.

In conclusion, this study provides evidence of volumetric and morphological alterations in the caudate of ADHD boys, with ADHD/+RD showing more extensive alterations than ADHD/-RD. The greater inward deformation or volume loss in ADHD/+RD may implicate widespread alterations in the corticostriatal networks that are involved in executive functions, attention and cognitive control. In contrast, volumetric and morphological alterations in the putamen may be similar in ADHD/-RD and ADHD/+RD suggesting similar degree of impairment in motor control in both groups. Overall, inward deformations in the striatum may implicate structural alterations in the cortical regions projecting to the striatum as well as disruption in the white matter tracts connecting the cortex to the striatum.

CHAPTER 4: Cortical Thickness Analysis

4.1 Introduction

As noted in Chapter 1, numerous structural MRI studies have implicated cortical and sub-cortical brain regions in ADHD (Friedman & Rapoport, 2015; Krain & Castellanos, 2006; Nigg, 2013). This includes reduced total brain volume in children with ADHD relative to HC (Krain & Castellanos, 2006) as well as volume reductions in the prefrontal cortex (PFC), inferior parietal cortex (IPC), superior parietal cortex (SPC), anterior cingulate cortex (ACC), premotor cortex and motor cortex (Friedman & Rapoport, 2015; Krain & Castellanos, 2006; Nigg, 2013). While earlier studies focused on volume measures, advances in neuroimaging processing tools have allowed researchers to extend volume measurements into surface area of certain structures and the thickness of cortex (Worker et al., 2014). These methods are referred to as surface-based morphometry (SBM).

SBM is a computational technique that allows reconstruction of 3D cortical surface models from structural MRI volume scans. Through this process it is possible to generate a surface map with vertices representing the surface area or thickness of the cortex. Cortical surface area and cortical thickness measures are a substantial improvement over conventional volume measures because it allows a direct measure of the cortical ribbon of the cerebrum. Since volume measurement is a product of surface area and cortical thickness, it is possible that subtle alterations in cortical thickness may not be reflected to the same degree as an alteration in the volume measurement. Therefore, it can be argued that cortical thickness measurements may be more

sensitive in detecting subtle cortical pathologies compared to volume measurements. Furthermore, studies comparing volume based methods to SBM have shown that both approaches provide similar results because of the inherent relationship between thickness and volume, but thickness measurements have been shown to be more sensitive at detecting alterations compared to volume based measures (Hutton, Draganski, Ashburner, & Weiskopf, 2009). Though, cortical thickness is a physical measurement between two points (i.e., a point along the pial surface and its nearest point at the gray and white matter interface), it is thought to reflect underlying neuronal density or size of neuronal cell bodies (Dale, Fischl, & Sereno, 1999; Worker et al., 2014). Therefore, reduced cortical thickness may imply loss of neurons or degradation of neuronal cell bodies.

Regarding ADHD, there are several published studies that have investigated alterations in cortical thickness in children with ADHD. In general, these studies have reported significant thinner cortex in ADHD children compared to HC in multiple different cortical regions, including PFC, temporal cortex (TC), PC, and ACC (Almeida et al., 2010; Almeida Montes et al., 2013; Batty et al., 2010; Hoekzema et al., 2012; Narr et al., 2009; M. G. Qiu et al., 2011). However, the findings of these studies have been highly variable in terms of the localization of clusters of thinner cortex. The inconsistencies may be largely due to variability in the heterogeneity of the samples used by these studies and tend to include comorbid conditions such as RD, ODD/CD, anxiety disorder and/or depression.

As commented earlier, RD is one of the most common comorbid conditions in ADHD children with ADHD; however, most studies investigating ADHD fail to account

for RD, which is especially evident in structural MRI studies. While neuropsychological studies have shown relatively greater impairments of multiple cognitive domains in ADHD/+RD relative to ADHD/-RD (Chapter 1), to date there have been no published studies directly investigating the influence of comorbid RD on the morphology of cortical mantle in children with ADHD. Alterations in multiple cortical regions particularly in the Brocca's area, Wernicke's area, and left fusiform gyurs of individuals with RD, which are associated with reading skills, have been reported (Norton et al., 2015; Sun et al., 2010; Vandermosten et al., 2012). Therefore, it is likely that alterations in these regions may be uniquely present in ADHD/+RD. The purpose of this investigation was to identify significant differences in cortical thickness between ADHD boys with and without a reading disability relative to HC individuals. Based on prior reports of thinner cortex in children with ADHD, we hypothesize that ADHD/-RD boys will demonstrate significant thinner cortex in the PFC, PC and ACC areas. We further hypothesize that ADHD/+RD boys will show thinner cortex in the PFC, PC and ACC to a greater extent as well as thinner cortex in additional regions of the brain that are associated with RD.

4.2 Methods

4.2.1 Sample Characteristics

Similar to Chapter 3, 37 boys with ADHD diagnosis (22 ADHD/-RD and 15 ADHD/+RD) and 29 age-matched HC boys were used to investigate differences in cortical thickness between subject groups. The diagnosis procedure and inclusion/ exclusion criteria for ADHD and HC are detailed in Chapter 2. Briefly, DSM-IV diagnosis of ADHD was based on clinical neuropsychologists' assessment using the K-SADS,

Conner's parent/teacher ratings and DBD parent ratings. The diagnosis of RD was based on WIAT-III assessment and was determined using normalized discrepancy scores from WIAT-III. The ADHD boys consisted of 27 combined type ADHD (13 ADHD/-RD and 14 ADHD/+RD) and 10 inattentive type ADHD (9 ADHD/-RD and 1 ADHD/+RD). Regarding comorbid conditions, the ADHD/-RD subgroup included 7 participants with an oppositional defiance disorder (ODD), whereas the ADHD/+RD included 6 participants with ODD and 1 participant with a separation anxiety disorder. The summary of sample characteristics is tabulated in Table 4.1.

Table 4.1: Sample characteristics

		HC	ADHD/-RD	ADHD/+RD	*Main Term p-value*
Sample Size		29	22	15	
Age (SD)		10.4 (2.3)	11.1 (2.4)	9.6 (2.4)	n.s.
Full Scale IQ (SD)		107 (14)	107 (18)	104 (16)	n.s.
Verbal IQ (SD)		106 (14)	110 (19)	102 (17)	n.s.
Performance IQ (SD)		106 (14)	103 (14)	105 (13)	n.s.
ADHD Subtype	Combined	-	11	14	-
	Innattentive	-	8	1	-
Oppositional Defiane Disorder		-	7	6	-
Conner's Inattention (SD)		-	62 (13)	60 (9)	n.s.
Conner's Hyperactivity (SD)		-	67 (13)	72 (13)	n.s.
Word Reading Norm (SD)		102 (9)	106 (11)	84 (16)[a]	<0.001
Pseudoword Decode Norm (SD)		102 (9)	106 (11)	82 (17)[a]	<0.001
Spelling Norm (SD)		103 (14)	101 (9)	85 (13)[a]	<0.001

[a]Post-hoc results show significant differences compared to both ADHD/-RD and HC ($p \leq 0.001$)

4.2.2 Post-processing and Generating Cortical Thickness maps

Freesurfer image analysis tool (http://freesurfer.net/fswiki/FreeSurferWiki) was used to generate 3D cortical surface models and compute cortical thickness maps. High-spatial resolution 3D T_1-weighted MRI images were used to reconstruct 3D cortical surface and generate their cortical thickness maps. Data acquisition and basic pre-processing steps are discussed in Chapter 2. Briefly, multiple high-spatial resolution 3D T_1-weighted MRI scans collected for each subject were quality checked, NU corrected, de-noised and averaged. These corrected and averaged high-spatial resolution 3D T_1-weighted MRI images were used to generate and analyze cortical thickness differences between groups.

The reconstruction of cortical surface and computing cortical thickness maps involved multiple steps and are well described in prior publications (Dale et al., 1999; Dale & Sereno, 1993; Fischl & Dale, 2000; Fischl, Liu, & Dale, 2001; Fischl et al., 2002; Fischl, Salat, et al., 2004; Fischl, Sereno, & Dale, 1999; Fischl, Sereno, Tootell, & Dale, 1999; Fischl, van der Kouwe, et al., 2004; Han et al., 2006; Jovicich et al., 2006; Segonne et al., 2004). The first step was skull stripping using a hybrid watershed/surface deformation procedure (Segonne et al., 2004). Since the defaults were not optimal in our sample, the skull stripping step were repeated multiple times with different watershed thresholds (threshold values = 3, 5, 7, 9, 11, 13, 15) and the most optimal de-skulled image was selected for further processing. The skull stripped images were Talairach transformed using an automated approach and segmented to extract white matter and sub-cortical gray matter structures (Fischl et al., 2002). The output of the segmentation was visually inspected and corrected for misclassification of

white matter by either adding control points for white matter that was labeled gray matter or by filling in voxels on the white matter segmented image. The gray matter/pial boundaries were also corrected by removing non-brain tissue voxels that were included as gray matter. Once the gray/white boundary and the gray/pial boundary were corrected, they underwent tessellation of the gray matter white matter boundary, automated topology correction (Fischl et al., 2001), and surface deformation following intensity gradients to optimally place the gray/white and gray/cerebrospinal fluid borders at the location where the greatest shift in intensity defines the transition to the other tissue class (Dale et al., 1999). Once the cortical models are complete, a number of deformable procedures were performed including surface inflation (Fischl, Sereno, & Dale, 1999), registration to a spherical atlas which utilized individual cortical folding patterns to match cortical geometry across subjects (Fischl, Sereno, Tootell, et al., 1999), parcellation of the cerebral cortex into units based on gyral and sulcal structure (Desikan et al., 2006), and creation of a variety of surface based measures including cortical thickness maps. This method uses both intensity and continuity information from the entire three dimensional MR volume in segmentation and deformation procedures to produce representations of cortical thickness, which is calculated as the closest distance from the gray/white boundary to the gray/CSF [pial surface] boundary at each vertex on the tessellated surface (Fischl & Dale, 2000). The maps were created using spatial intensity gradients across tissue classes. Therefore, the measurements do not depend only on absolute signal intensity. Furthermore, the maps are not limited by the original voxel resolution and are, therefore, capable of detecting submillimeter differences between groups. This approach of cortical thickness measurements have

been validated against histological analysis (Rosas et al., 2002) and manual measurements (Kuperberg et al., 2003). In addition, Freesurfer's data processing procedures have been demonstrated to show good test-retest reliability across scanner manufacturers and across field strengths (Han et al., 2006).

Two approaches have been used to conduct statistical comparison of cortical thickness data. First approach is a region of interest (ROI) analysis, where cortical thickness measures over ROI's are averaged and used as dependent variables in the statistical analysis. Second approach is a vertex-by-vertex analysis, where local cortical thickness at each vertex on the surface of the cerebrum is statistically analyzed. The ROI based approach is simpler to apply; however, has the disadvantage of being less sensitive for detecting differences within ROI's where potentially mean cortical thickness values between groups are in opposite directions. As an alternative, a vertex-by-vertex analysis approach was also chosen. In order to conduct vertex-by-vertex analyses, the cortical thickness surface map of each subject have to be in standard coordinate system referred to as template space. This is necessary to ensure that the vertices being compared represent the same location of the brain in all subjects. In this study, a sample specific template was created since the study uses data from children and adolescents and the existing freesurfer template is based on adult data. The template was created using HC data from the sample. As a first step for template creation, cortical surfaces of each HC were co-registered to the freesurfer template, using surface based co-registration algorithm. The co-registered cortical surfaces where then averaged to create a sample specific template cortical surface. Following template creation, cortical surface from subjects in the sample were co-registered to the sample

specific template to transform them into a common standard space. The cortical thickness maps were also resampled to conform to standard space. The resampled cortical thickness maps were smoothed using a 5mm FWHM smoothing kernel. The smoothed cortical thickness maps were used to conduct vertex-by-vertex comparison of cortical thickness across groups.

4.2.3 Statistical Analysis

Group differences in age, full scale, performance and verbal IQ, reading performance (word reading, pseudoword decoding, and spelling normed scores), and Conner's ADHD symptom scores (inattention and hyperactivity scores) were assessed using one-way analysis of variance (ANOVA; SPSS version 22, IBM Corp.) tests with subject-group (ADHD/-RD, ADHD/+RD and HC) as the main effect term followed by post-hoc analyses of planned contrast comparisons in the case when the group term reaches significance (i.e., $p < 0.05$).

Statistical analyses of differences between groups in the cortical thickness values along the surface map were conducted using freeSurfer's glmfit tool (Fischl, Sereno, & Dale, 1999; Fischl, Sereno, Tootell, et al., 1999). A multivariate generalized linear model (GLM) was used to assess group differences on the cortical thickness maps on a vertex-by-vertex basis and covarying for age and ICV. ICV was included as a covariate to account for differences in the head size between subjects as ICV was significantly correlated with the mean cortical thickness. The random field theory (RFT) based cluster-wise multiple comparison correction implemented in SurfStat (http://www.math.mcgill.ca/keith/surfstat/) and Matlab (The MathWorks Inc.) was

employed and an RFT corrected cluster-level p-value of 0.05 was used to determine significant clusters.

4.3 Results

4.3.1 Subject-group Characteristics

There were no significant differences between subject groups in age ($F_{2,63}$ = 2.13, p = 0.13), full scale IQ ($F_{2,63}$ = 0.24, p = 0.79), verbal IQ ($F_{2,63}$ = 0.92, p = 0.41) or performance IQ ($F_{2,63}$ = 0.46, p = 0.63). For Conner's' composite scores, there was no significant difference between ADHD/-RD and ADHD/+RD in inattention score ($F_{1,35}$ = 0.17, p = 0.69) or hyperactivity score ($F_{1,35}$ = 1.11, p = 0.30). As expected on the WIAT-III reading scores, there was a significant group effect on Word Reading normed scores ($F_{2,63}$ = 12.49, p < 0.001), Pseudoword Decoding normed scores ($F_{2,63}$ = 21.79, p < 0.001), and Spelling normed scores ($F_{2,63}$ = 10.86, p < 0.001) with post hoc analyses showing significantly worst performance in the ADHD/+RD group compared to both ADHD/-RD and HC on these three reading scores (p ≤ 0.001) and no significant differences between ADHD/-RD and HC. Regarding ICV, there were no significant differences between subject groups in ICV ($F_{2,62}$ = 0.99, p = 0.38) after controlling for age. Table 4.1 includes a summary of the results.

4.3.2 Cortical Thickness Analysis

ADHD/-RD Vs. HC: GLM analysis was conducted comparing cortical thickness measurement at each vertex along the cortical surface between ADHD/-RD and HC. Age and ICV were used as covariates in the analysis. A cluster-wise RTF based

approach for multiple comparison corrections was used and only clusters with $p < 0.05$ after RFT correction were reported as being significant. The analysis showed no significant clusters of thinner cortex or thickening in ADHD/-RD relative to HC.

ADHD/+RD Vs. HC: Using the similar analysis approach as above, the results showed multiple significant clusters of thinner cortex in ADHD/-RD relative to HC (Figure 4.1; Table 4.2). These clusters were localized in the right ACC, right middle TC, right PC, right precuneus/posterior cingulate, right insula and Wernicke's area. The mean cortical thicknesses for each cluster of interest are tabulated in Table 4.2. Additionally, there were no significant clusters of cortical thickening in ADHD/+RD relative to HC.

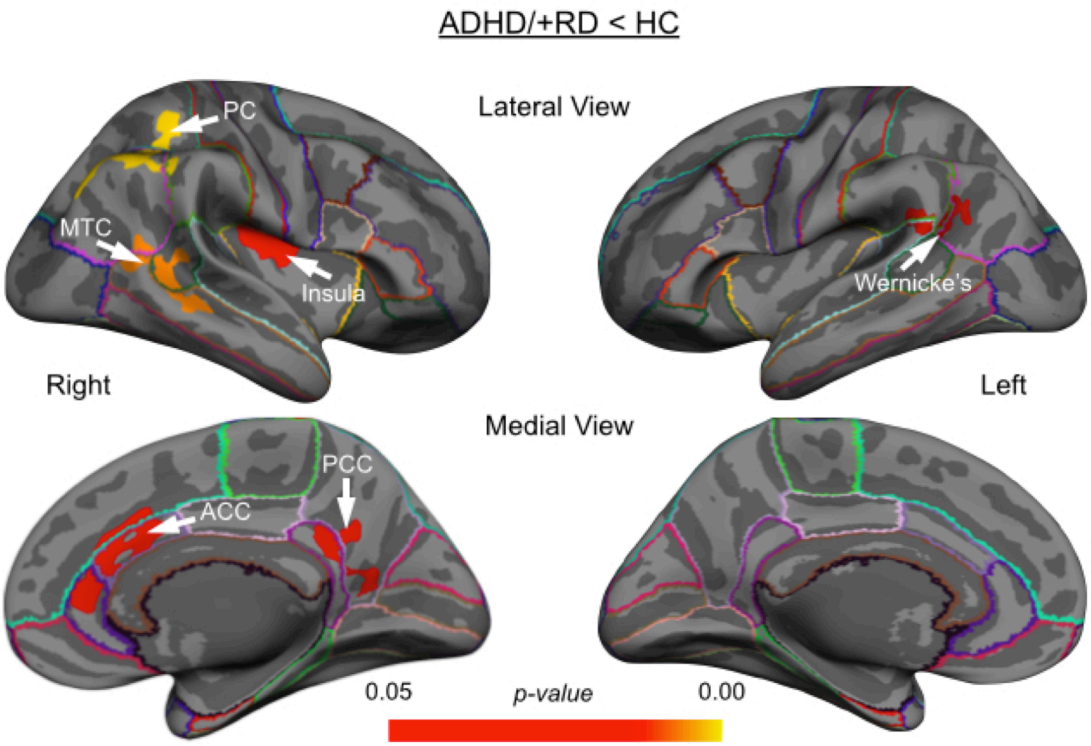

Figure 4.1: Results showing thinner cortex in ADHD/+RD relative to HC. Clusters of significantly thinner cortex are observed in the right PC, right MTC, right insula, right ACC, right PCC/precuneus and Wernicke's area. PC = parietal cortex, MTC = middle temporal cortex, ACC = anterior cingulate cortex, PCC = posterior cingulate cortex.

Table 4.2: Group differences in cortical thickness measurement between ADHD/-RD, ADHD/+RD and HC

Contrast	Region	Side	Cluster Size	$P_{rtf\text{-}cluster}$	Mean Thickness (SD) in mm		
					HC	ADHD/-RD	ADHD/+RD
ADHD/+RD < HC	Parietal cortex	Right	2716	<0.0001	3.18(0.22)	3.02(0.15)	2.82(0.21)
	Posterior Temporal cortex	Right	1559	<0.0001	3.46(0.21)	3.34(0.22)	3.17(0.21)
	Anterior Cingulate cortex	Right	1524	0.006	3.33(0.29)	3.27(0.26)	2.92(0.42)
	Precunus	Right	1000	0.008	3.39(0.19)	3.26(0.21)	3.12(0.26)
	Insula	Right	1443	0.005	3.48(0.23)	3.32(0.27)	3.11(0.33)
	Precentral gyrus	Right	920	0.014	2.04(0.17)	1.94(0.18)	1.77(0.15)
	Wernick's Area	Left	1191	0.003	3.23(0.23)	3.11(0.22)	2.89(0.21)
	Parietal cortex	Left	852	0.04	3.09(0.26)	2.96(0.19)	2.77(0.26)
	Premotor cortex	Left	738	0.05	3.26(0.22)	3.06(0.19)	2.93(0.34)
ADHD/+RD < ADHD/-RD	Anterior Cingulate cortex	Right	1191	0.04	3.32(0.33)	3.29(0.27)	2.89(0.52)
	Supramarginal cortex	Right	1919	<0.001	2.89(0.27)	2.92(0.28)	2.62(0.25)
	Postcentral gyrus	Right	991	0.03	1.87(0.15)	2.05(0.24)	1.85(0.15)
	Wernick's Area	Left	871	0.025	3.32(0.28)	3.32(0.28)	2.96(0.18)
	Fusiform gyrus	Left	718	0.04	3.02(0.28)	3.13(0.27)	2.88(0.18)

ADHD/+RD Vs. ADHD/-RD: Comparing to ADHD/-RD, ADHD/+RD showed multiple significant clusters of thinner cortex (Figure 4.2; Table 4.2). These clusters were localized in the right ACC, Wernicke's area and left fusiform gyrus. Lastly, there were no significant clusters of cortical thickening in ADHD/+RD relative to ADHD/-RD.

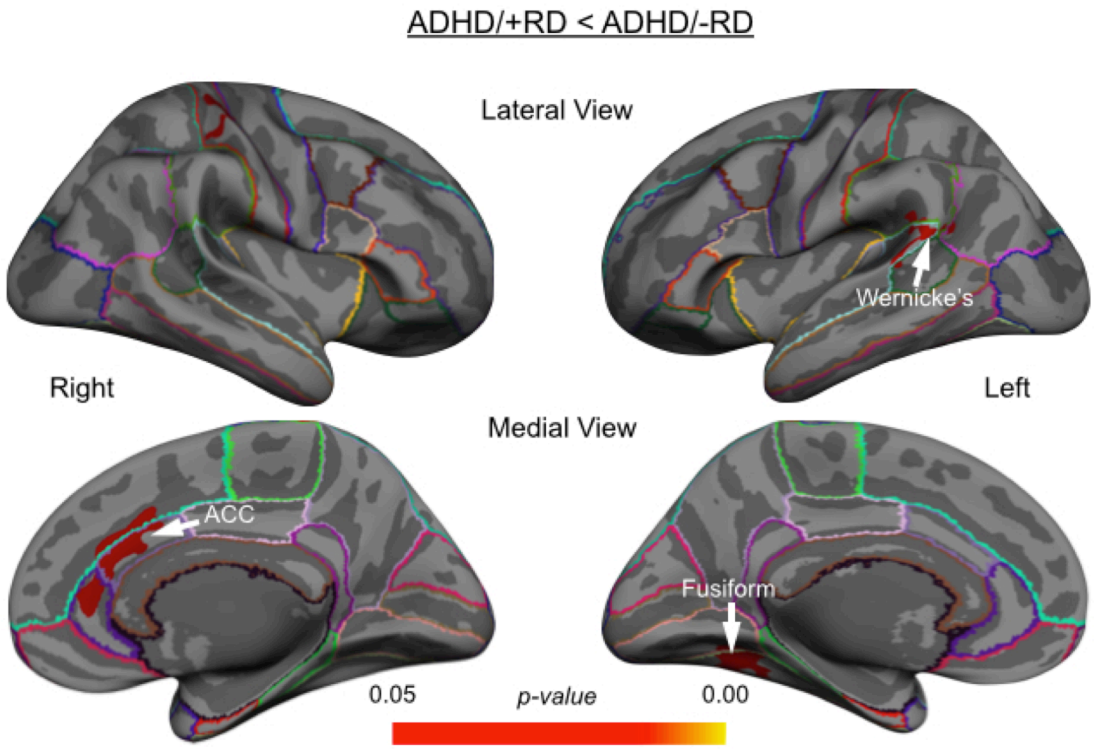

Figure 4.2: Results showing thinner cortex in ADHD/+RD relative to ADHD/-RD. Clusters of significantly thinner cortex are observed in the right ACC, Wernicke's area and left fusiform gyrus. ACC = anterior cingulate cortex.

4.4 Discussion

To our knowledge, this is the first study reporting significant differences in the thickness of the cerebral cortex between boys with and without a comorbid RD condition and HC. In contrast to the hypothesis, there were no significant clusters in cortical thickness measurement differentiating ADHD/-RD from HC. However, when ADHD/+RD were compared to HC, there were significant clusters of thinner cortex in multiple cortical areas (Figure 4.1). Furthermore, ADHD/+RD also showed significant clusters of thinner cortex in multiple cortical areas when compared to ADHD/-RD boys (Figure 4.2). These findings are important in demonstrating, for the first time, differences in cortical thickness measurement that may be influenced by the presence of comorbid RD in boys with ADHD.

ADHD/+RD boys showed significant clusters of thinner cortex in right ACC, bilateral PC, right precuneus/posterior cingulate, right insula and Wernicke's area (Figure 4.1). These observations are consistent with previous studies showing thinner cortex in children with ADHD (Almeida et al., 2010; Almeida Montes et al., 2013; Batty et al., 2010; Hoekzema et al., 2012; Narr et al., 2009; M. G. Qiu et al., 2011); however, these studies did not exclusively rule out ADHD subjects with a comorbid RD condition suggesting that prior observation of thinner cortex in ADHD may be confounded by the presence of comorbid RD condition in their samples. Furthermore, the ACC and PC known to be associated with cognitive functions including response inhibition and attention respectively, which are shown to be impaired in children with ADHD/+RD relative to HC (Barkley, 1997; Nigg & Casey, 2005; Sonuga-Barke, 2005). These finding suggest that alterations in cortical thickness observed in ADHD/+RD may underlie the

greater degree of impairments seen in response inhibition and attention in children with ADHD/+RD.

On the other hand, when compared to ADHD/-RD, ADHD/+RD boys show significant clusters of thinner cortex in the right ACC, Wernicke's area and left fusiform gurus (Figure 4.2). While the ACC is associated with response inhibition, the fusiform gyrus and Wernicke's area are associated with reading, particularly orthographic processing (Vandermosten et al., 2012). These findings suggest that ADHD/+RD may have additional alterations in the regions associated with reading abilities, which may impede their ability to attain the appropriate reading skills.

Surprisingly, relative to HC, ADHD/-RD did not show any significant difference in cortical thickness measurements. This is inconsistent with the hypothesis of observing significant thinner cortex in ACC, PC and dPFC. However, despite lack of significant finding, qualitative comparison of mean cortical thickness from clusters of significant thinning observed in ADHD/+RD relative to HC (Table 4.2) shows that ADHD/-RD group thinner cortex relative to HC. This suggests that the effect is small and the current sample does not have adequate power to detect these differences.

Overall, the finding of this investigation clearly demonstrates that boys with ADHD have thinner cortex in regions that are implicated in ADHD by previous studies, with ADHD/+RD boys showing greater degree of thinner cortex than ADHD/-RD. Furthermore, ADHD/+RD boys show thinner cortex areas associated with reading and response inhibition when compared to ADHD/-RD. Together these results provide evidence that boys with ADHD/+RD have greater alterations in the cortical morphology

with additional alterations in regions associated with RD, which may differentiate them from boys with ADHD/-RD.

A limitation of the current study is the borad age range of sample (6 to 14 years). Developmentally, the cerebral cortex is highly dynamic during this age range. Therefore, it is likely that differences in the developmental trajectories between groups can confound the results observed above. The lack of findings in the ADHD/-RD but not ADHD/+RD relative to HC could potentially be, in part, due to differences in the developmental trajectories between of ADHD/-RD and ADHD/+RD. Longitudinal studies are, therefore, required to elucidate if ADHD/-RD and ADHD/+RD have different developmental profiles.

In conclusion, the study provides evidence of significant influence of comorbid RD in the cortical morphology of boys with ADHD with ADHD/+RD boys showing greater degree of cortical alterations than ADHD/-RD boys. These cortical differences differentiate ADHD/+RD from ADHD/-RD and may underpin the severity of cognitive impairments observed in ADHD/+RD.

CHAPTER 5: DTI Analysis

5.1 Introduction

Investigations of structural alterations in ADHD relative to HC are not limited to gray matter regions. Several studies have been conducted to assess white matter architecture and neuropathology in children with ADHD (van Ewijk et al., 2012). Prior studies examining white matter volume have consistently reported reduced total white matter volume in ADHD children along with bilateral volume reduction in all four lobes of the cerebrum (Castellanos et al., 2002; Kates et al., 2002; McAlonan et al., 2007). One study found significant volume reduction along the superior and inferior longitudinal fasciculi, corpus callosum and cerebellum (McAlonan et al., 2007). These findings provide preliminary evidence of altered white matter in children with ADHD, which may underpin the dysfunction in corticostriatal connectivity implicated in ADHD. However, it is important to note that there is a lack of evidence to support a clear relationship between white matter volume and DTI metrics of white matter integrity/pathology suggesting that white matter volume reduction may not be directly associated with white matter integrity or pathologies (Canu et al., 2010; Fjell et al., 2008; Hugenschmidt et al., 2008).

Diffusion tensor imaging (DTI) is another structural MRI technique that is specific in assessing white matter neuropathologies. As discussed in Chapter 2, DTI exploits local diffusion properties of water molecules in the brain to characterize white matter structure by quantifying the directionality and magnitude of the anisotropy of water diffusion within the tissue (Basser et al., 1994). The white matter structure is

characterized using various indices of DTI including Fractional Anisotropy (FA), Axonal Diffusivity (DA) and Radial diffusivity (DR). FA quantifies the degree of anisotropy of water diffusion along the fiber tract and ranges from 0 in regions with free diffusion (fully isotropic) such as CSF to 1 in regions with restricted diffusion (fully anisotropic) such as white matter (van Ewijk et al., 2012). FA is the most commonly reported outcome measurement in DTI studies and has been implicated in many disorders and neurological conditions. The interpretation of an alteration in FA in pathology is, however, complex due to multiple factors that can influence alterations in FA. These include alterations in axonal density, presence of crossing fibers, neuronal branching, myelin injury, myelin loss and edema (van Ewijk et al., 2012). For example, a decrease in FA in a fiber bundle can be due to an increase in the number of crossing fibers or due to myelin injury/loss giving rise to decreased anisotropy of water diffusion. Consequently, the interpretation of differences in FA is typically viewed as reflecting the integrity of white matter tracks. On the flip side, DA and DR values tend to provide relatively greater insight about the neurobiology of the fiber tracts. DA reflects the diffusion of water along the direction of the fiber tract and is represented by the primary eigenvalue (λ_1); whereas, DR reflects the diffusion of water perpendicular to the direction of the fiber tract and is represented as the average of second and third eigenvalues ($\lambda_1+\lambda_1/2$). An alteration in FA can occur due to an alteration in DA or an alteration in DR or a combination of both. For instance, a decrease in FA with a decrease in DA and a negligible difference in DR may suggest the presence of axonal damage or degeneration (Alexander, Lee, Lazar, & Field, 2007; Song et al., 2003). In contrast, a decrease in FA accompanied by an increase in DR and minimal difference in

DA may suggest decreased myelination (Alexander et al., 2007; Song et al., 2002). Therefore, investigating DA and DR in conjunction with FA can provide greater understanding of the neurobiology of the white matter abnormalities.

Regarding DTI studies in ADHD, several groups have reported somewhat inconsistent atypical FA values in multiple white matter regions (Ashtari et al., 2005; Davenport et al., 2010; Kobel et al., 2010; Konrad et al., 2010; Nagel et al., 2011; M. G. Qiu et al., 2011; Silk et al., 2009). Some have reported decreased FA values in the bilateral superior longitudinal fasciculus (SLF), bilateral anterior corona radiata (ACR), bilateral uncinate fasciculus (UF), bilateral cerebellum and right inferior longitudinal fasciculus (ILF) of ADHD children (Ashtari et al., 2005; Kobel et al., 2010; Konrad et al., 2010; Nagel et al., 2011; M. G. Qiu et al., 2011). While others have reported increased FA values in the right SLF, right posterior corona radiata (PCR), bilateral ACR, bilateral ILF and left UF of ADHD children (Davenport et al., 2010; Kobel et al., 2010; Konrad et al., 2010; Silk et al., 2009). One of the potential sources of variability in the findings of these studies may be due to the variability in the heterogeneity of the samples used by these studies. Most of these studies tend to include comorbid conditions such as RD, ODD/CD, anxiety disorder and/or depression, which may influence the results of the studies. In addition, the variability of the findings may also be, in part, due to differences in data acquisition, pre-processing and analysis methodologies (van Ewijk et al., 2012).

As discussed in Chapter 1, RD is one of the most common comorbid conditions in children with ADHD. However, most studies investigating ADHD fail to account for RD, which is especially evident in structural MRI studies. DTI investigations into the correlates of white matter alterations in children with RD have reported significant

decrease in FA in bilateral SFL and left arcuate fasciculus (AF) in children with RD relative to HC (Carter et al., 2009; Rimrodt, Peterson, Denckla, Kaufmann, & Cutting, 2010; Steinbrink et al., 2008). Interestingly, atypical FA in the SLF is common for both ADHD and RD groups. The SLF connects the parietal regions to the frontal regions forming frontoparietal networks that sub-serve function of attention. Since children with ADHD and RD are known to present impairment in attention, it is not surprising to see the SLF implicated in both groups. In contrast, the left AF, which connects the Wernicke's area to the Brocca's area, may be a unique to RD.

While neuropsychological studies have shown relatively greater impairments of multiple cognitive domains in ADHD/+RD relative to ADHD/-RD (Chapter 1), to date there have been no published studies directly investigating the influence of comorbid RD on the white matter structure in children with ADHD. Therefore, the purpose of this investigation was to identify significant differences in FA between ADHD boys with and without a reading disability relative to HC individuals. Based on prior reports of atypical FA in children with ADHD or RD, it is hypothesize that ADHD/-RD boys will demonstrate significantly decreased FA in the SLF, ACR, UF and ILF. It is further hypothesize that ADHD/+RD boys will show decreased FA in SLF and left AF with SLF showing more widespread alterations relative to ADHD/-RD. Further, the study also assesses DA and DR to elucidate the underlying derivative of FA abnormality. It is hypothesized that FA differences will be driven by differences in the DA but not DR implicating that abnormalities in the white matter structure may be due to alterations in the tissue architecture rather than myelination.

5.2 Methods

5.2.1 Sample Characteristics

To assess differences in diffusion parameters (FA, DA and DR) between subject groups, DTI data was acquired in 37 boys with ADHD diagnosis (22 ADHD/-RD and 15 ADHD/+RD) and 27 age-matched HC boys. The diagnosis procedure and inclusion/ exclusion criteria for ADHD and HC are detailed in Chapter 2. Briefly, DSM-IV diagnosis of ADHD was based on clinical neuropsychologists' assessment using the K-SADS, Conner's parent/teacher ratings and DBD parent ratings. The diagnosis of RD was based on WIAT-III assessment and was determined using normalized discrepancy scores from WIAT-III. The ADHD boys consisted of 27 combined subtype ADHD (13 ADHD/-RD and 14 ADHD/+RD) and 10 predominantly inattentive subtype ADHD (9 ADHD/-RD and 1 ADHD/+RD). Regarding other comorbid conditions, the ADHD/-RD subgroup included 7 participants with an ODD, whereas the ADHD/+RD included 6 participants with ODD and 1 participant with a separation anxiety disorder. The summary of sample characteristics is tabulated in Table 5.1.

Table 5.1: Sample characteristics

		HC	ADHD/-RD	ADHD/+RD	*Main Term p-value*
Sample Size		29	22	15	
Age (SD)		10.1 (2.3)	11.1 (2.4)	9.6 (2.4)	n.s.
Full Scale IQ (SD)		105 (12)	107 (18)	104 (16)	n.s.
Verbal IQ (SD)		105 (13)	110 (19)	102 (17)	n.s.
Performance IQ (SD)		104 (12)	103 (14)	105 (13)	n.s.
ADHD Subtype	Combined	-	11	14	-
	Innattentive	-	8	1	-
Oppositional Defiane Disorder		-	7	6	-
Conner's Inattention (SD)		-	62 (13)	60 (9)	n.s.
Conner's Hyperactivity (SD)		-	67 (13)	72 (13)	n.s.
Word Reading Norm (SD)		102 (10)	106 (11)	84 (16)[a]	<0.001
Pseudoword Decode Norm (SD)		102 (9)	106 (11)	82 (17)[a]	<0.001
Spelling Norm (SD)		102 (15)	101 (9)	85 (13)[a]	<0.001

[a]Post-hoc results show significant differences compared to both ADHD/-RD and HC ($p \leq 0.001$)

5.2.2 Post-processing of DTI Data

Data acquisition protocol and basic pre-processing steps of the DTI data are discussed in Chapter 2. Briefly, diffusion weighted images (DWI) for each subject included 3 volumes at b=0 s/mm^2 and 55 diffusion sensitive volumes at b=700 s/mm^2. The DWIs were quality checked, de-noised and eddy current corrected. Diffusion tensors were computed using weighted least squared fitting and FA, AD and RD maps were generated. The FA, AD and RD maps were further processed to conduct group comparisons.

In the analysis of DTI indices, two types of analytic approaches can be used: ROI analysis and voxel based analysis (VBA). ROI based analysis allows investigation of specific tracks of interests by computing mean DTI indices within the specific tract which can then by compared between groups. However, ROI analysis has limited sensitivity to detect group differences because the measurement is averaged over a large region. On the other hand VBA allows comparison of DTI indices between groups on a voxel-by-voxel basis and is comparatively more sensitive to detect subtle differences in measurements localized within specific tracts. Therefore, VBA approach was chosen for investigating group differences between ADHD/-RD, ADHD/+RD and HC. In order to conduct VBA, the maps of DTI indices were further processed to normalize to a template space. The processing included white matter segmentation, template creation, normalization and smoothing.

Segmentation: In order to minimize partial volume effects and improve white matter coregistration, T_1-weighted images were segmented in gray matter, white matter and CSF tissue type image using the FSL's FAST algorithm. The FAST algorithm relies

on hidden Markov random field model and expectation-minimization algorithm to segment structural scans into various tissue types (Zhang, Brady, & Smith, 2001). The T_1-weighted structural scan was used for segmentation. First the structural scan was deskulled using FSL's BET algorithm (Smith, 2002). The deskulled images were then segmented to create binary images of gray matter, white matter and CSF. Once the binary white matter segmented images were generated of each subject, they were used to extract segmented maps of FA, DA and DR by multiplying the binary image with the respective maps of DTI indices.

Template Creation: To allow comparison of FA values between groups in VBA, it is necessary to normalize the FA maps to a standard template map so that each voxel approximate to the same location in the brain for all subjects. A study specific template was created using data from HC group to be used as a standard template map. Segmented FA map of each HC subject was normalized to an NIH pediatric white matter prior probability map (Fonov et al., 2011) using FSL's FLIRT algorithm (Jenkinson, Bannister, Brady, & Smith, 2002; Jenkinson & Smith, 2001). A 12-parameter affine transformation with a mutual information cost function was used to perform normalization. The normalized segmented FA maps of all HC subject were averaged to create a study specific FA template.

Normalization: Once the template was created, the segmented FA map of each subject in the sample was normalized to the study specific template using FSL's FLIRT algorithm with a 12-parameter affine transformation and mutual information cost function. In addition to the normalized FA maps, the transformation matrix was also

saved. The saved transformation matrix were then applied to AD and RD images respectively to normalize them.

Spatial Smoothing: The normalized segmented FA, AD and RD maps were smoothed using an isotropic Gaussian smoothing kernel with a FWHM of 6mm. The smoothed data were used in VBA to identify differences in FA, AD and RD measurements between groups.

5.2.3 Statistical Analysis

Group differences in age, full scale, performance and verbal IQ, reading performance (word reading, pseudoword decoding, and spelling normed scores), and Conner's ADHD symptom scores (inattention and hyperactivity scores) were assessed using one-way analysis of variance (ANOVA; SPSS version 22, IBM Corp.) tests with subject-group (ADHD/-RD, ADHD/+RD and HC) as the main effect term followed by post-hoc analyses of planned contrast comparisons for those group terms reaching significance (i.e., $p < 0.05$).

Statistical analyses of differences between groups in the segmented normalized FA, DA and DR maps were conducted using SPM (http://www.fil.ion.ucl.ac.uk/spm/). A multivariate generalized linear model (GLM) was used to assess group differences in the FA, DA and DR measurements on a voxel-by-voxel basis with age as a covariate. The comparison was restricted to all voxels with an FA > 0.2 in order to avoid inclusion of voxels that are localized in the gray matter regions. An FDR based multiple comparison correction was applied and only clusters with FDR corrected $p < 0.05$ were considered significant. If the clusters failed to survive FDR corrections, uncorrected

results are reported and clusters were considered significant if voxels within the cluster has an uncorrected $p < 0.05$ and a cluster size > 100 voxels. In order to investigate the potential mechanism that may underlie the differences in FA, VBA of DA and DR maps were conducted using GLM and were restricted to voxels encompassed within the clusters that were significant in the analysis of FA maps. Again, FDR correction for multiple comparisons was applied and if it failed uncorrected results are reported.

5.3 Results

5.3.1 Subject-group Characteristics

There were no significant differences between subject groups in age ($F_{2,61}$ = 2.05, p = 0.14), full scale IQ ($F_{2,61}$ = 0.25, p = 0.78), verbal IQ ($F_{2,61}$ = 0.90, p = 0.41) or performance IQ ($F_{2,61}$ = 0.58, p = 0.56). For Conner's' composite scores, there was no significant difference between ADHD/-RD and ADHD/+RD in inattention score ($F_{1,35}$ = 0.17, p = 0.69) and hyperactivity score ($F_{1,35}$ = 1.11, p = 0.30). As expected on the WIAT-III scores, there was a significant group effect on Word Reading normed scores ($F_{2,61}$ = 11.82, p < 0.001), Pseudoword Decoding normed scores ($F_{2,61}$ = 21.30, p < 0.001), and Spelling normed scores ($F_{2,61}$ = 10.07, p < 0.001) with post hoc analyses showing significantly worst performance in the ADHD/+RD group compared to both ADHD/-RD and HC on these three reading scores ($p \leq 0.001$) and no significant differences between ADHD/-RD and HC. Refer to Table 5.1 for summary of the results.

5.3.2 White Matter Analysis of DTI Measures

ADHD/-RD Vs. HC: GLM analysis was conducted comparing the FA measurement at each voxel along the white matter fiber tracks covering the whole brain between ADHD/-RD and HC. Age was used as covariates in the analysis. Uncorrected results showed multiple clusters of significant increase in FA in ADHD/-RD relative to HC (Figure 5.1). The clusters were localized in the left posterior corona radiata (PCR), right SLF and bilateral ACR (Table 5.2). However, there were no significant group differences in FA after FDR correction. There were no significant clusters of decreased FA between ADHD/-RD relative to HC. Regarding the DA measures, GLM analysis comparing AD measurement in the above clusters showed significant uncorrected increase in DA values in all the above clusters, which did not survive FDR correction, in ADHD/-RD relative to HC (Table 5.2). In contrast DR measurements were not significantly different between the two groups.

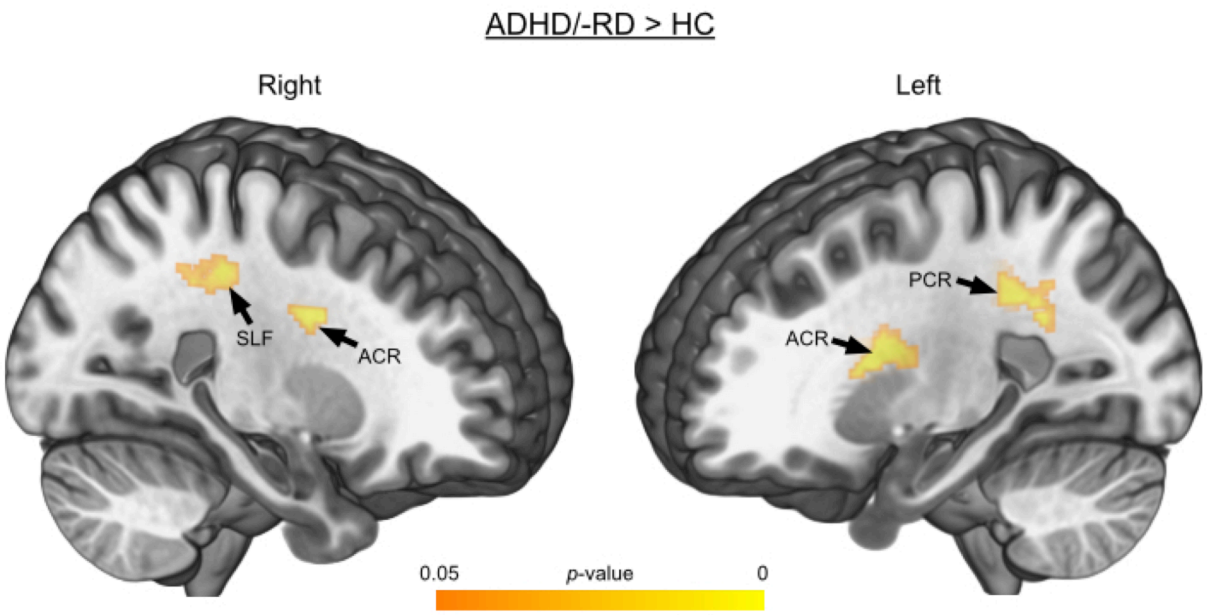

Figure 5.1: Results of FA analysis between ADHD/-RD and HC. Compared to HC, ADHD/-RD show significant clusters of increased FA in bilateral ACR, right SLF and left PCR. FA = fractional anisotropy, ACR = anterior corona radiata, PCR = posterior corona radiata, SLF = superior longitudinal fasciculus.

Table 5.2: Group differences in FA and DA measurements between ADHD/-RD, ADHD/+RD and HC.

Comparison	Location	Side	FA			DA		
			Cluster Size (Voxels)	t	Uncorrected *p*	Cluster Size (Voxels)	t	Uncorrected *p*
ADHD/-RD > HC	Anterior Corona Radiata	Right	214	3.27	0.001	212	4.32	<0.001
	Superior Longitudinal Fasciculus	Right	132	2.93	0.002	83	3.08	0.002
	Anterior Corona Radiata	Left	142	3.22	0.001	123	4.18	<0.001
	Posterior Corona Radiata	Left	220	4.38	<0.001	203	4.99	<0.001
ADHD/+RD > HC	Posterior Corona Radiata	Right	203	2.75	0.003	173	5.36	<0.001
	Inferior Uncinate Fasciculus	Right	124	2.81	0.002	64	3.81	<0.001
	Superior Longitudinal Fasciculus	Right	202	3.70	<0.001	201	5.24	<0.001
	Anterior Corona Radiata	Left	375	3.39	0.001	360	5.75	<0.001

ADHD/+RD Vs. HC: Using a similar approach as above, the analysis showed multiple clusters of significant (uncorrected for multiple comparison) increase in FA in ADHD/+RD relative to HC (Figure 5.2). The clusters were localized in the right SLF, right PCR, right UF and left ACR (Table 5.2). However, there were no significant clusters of increased FA after FDR correction. There were no significant clusters of decreased FA between ADHD/+RD and HC. Regarding the DA measures, GLM analysis comparing AD measurement in the above clusters showed significant uncorrected increase in DA values in all the above clusters, which did not survive FDR correction, in ADHD/+RD relative to HC (Table 5.2). In contrast DR measurements were not significantly different between the two groups.

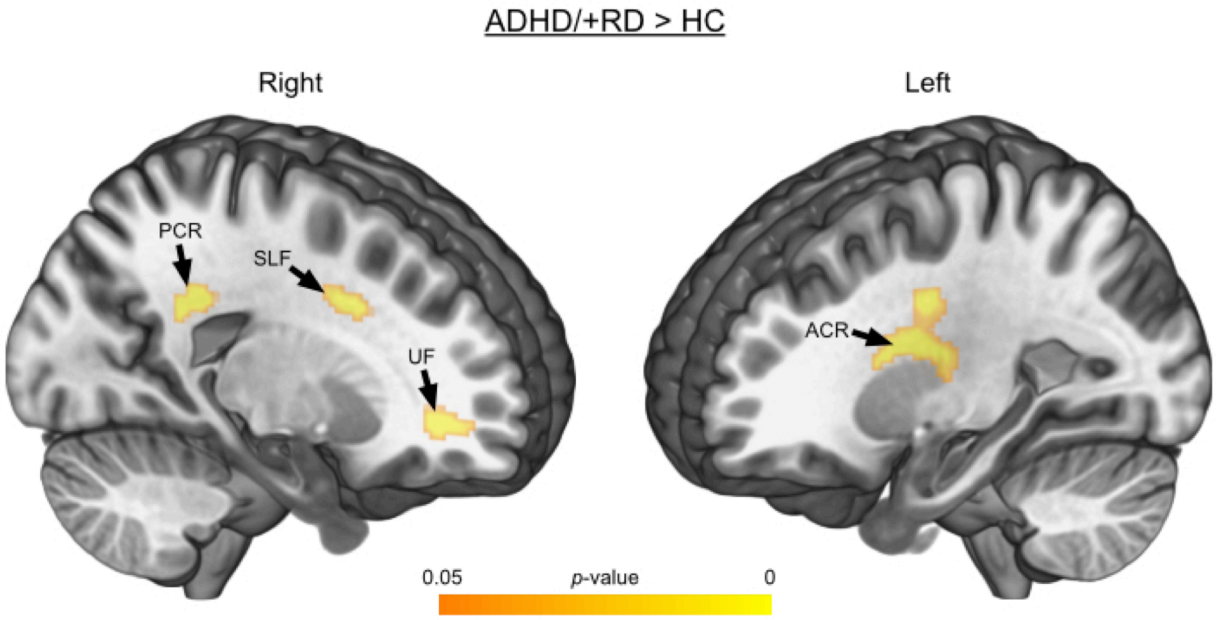

Figure 5.2: Results of FA analysis between ADHD/+RD and HC. Compared to HC, ADHD/-RD show significant clusters of increased FA in right SLF, right PCR, right UF and left ACR. FA = fractional anisotropy, ACR = anterior corona radiata, PCR = posterior corona radiata, SLF = superior longitudinal fasciculus, UF = uncinate fasciculus.

ADHD/+RD Vs. ADHD/-RD: Comparing to ADHD/-RD, ADHD/+RD showed no significant differences in the FA, DA or DR even when FDR correction was not applied.

5.4 Discussion

To our knowledge, this is the first study investigating significant differences in the DTI indices between boys with and without a comorbid RD condition and HC. Boys with ADHD/-RD showed significant uncorrected clusters of increased FA in the right SFL, bilateral ACR, and left PCR when compared to HC (Figure 5.1; Table 5.2). On the other hand, when ADHD/+RD were compared to HC, there were significant uncorrected clusters of increased FA in the left ACR, right SLF, right PCR and right UF (Figure 5.2; Table 5.2). However, none of the clusters survived multiple comparison correction. Evaluation of DA and DR maps demonstrate that the increase in FA is driven by the increase in AD (Table 5.2). Again, these clusters also did not survive multiple comparison correction. These results suggest that there is not significant effect of group on white matter structure.

The lack of significant group differences for FA, DA and DR may be due to small sample size, particularly of the ADHD subgroups. However, this is not surprising since most of the prior DTI studies in ADHD utilizing sample sizes similar to the current study have also reported uncorrected findings. Only two prior studies seem to have reported results corrected for multiple comparisons (Nagel et al., 2011; Silk et al., 2009). When conducting VBA, it has been advised that the results should be thresholded for minimum cluster size and corrected for multiple comparisons in order to minimize type I errors (Chumbley & Friston, 2009; Chumbley, Worsley, Flandin, & Friston, 2010).

Therefore, it is difficult to draw reliable conclusions based on uncorrected results. It is advisable to refrain from interpretation of results that do not survive multiple comparison. Thus, it is concluded that the sample in the present analysis may not have adequate power to detect group differences in DTI indices.

Another complicating factor associated with DTI analysis is artifact due to head motion. In addition to causing artifact in DTI data, head motion can pose significant problems in conducting group comparison when the patient group (eg. ADHD, tic disorder) is likely to have more head motion than the control group (van Ewijk et al., 2012). Head movement during scanning is difficult to correct and can negatively affect the outcome of statistical analysis of FA values (Jones & Cercignani, 2010; Ling et al., 2012). However, to minimize the effect of head motion in the present study, an automated algorithm to control DTI data quality was employed. The algorithm uses slice-wise and volume-wise correlations to identify and remove volume (from the series of gradient sensitive volumes acquired as part of a subject's DTI sequence) with head motion as well as other scanner-associated artifacts. Therefore, the impact of artifacts on statistical analysis is expected to be minimum.

In conclusion, the study provides no evidence of distinctive alterations in white matter architecture in boys with ADHD with and without comorbid RD. It is likely that this study is under powered and future studies with larger sample sizes are needed to identify significant differences in FA between ADHD boys with and without a reading disability relative to HC individuals.

CHAPTER 6: Conclusions, Implications, Limitation and Future Directions

6.1 Conclusion

ADHD is a neurodevelopmental disorder that is highly heterogeneous in symptomatology, often complicated by the presence of one or more comorbid conditions. The commonly occurring comorbid condition in children with ADHD include CD/ODD, anxiety disorder, depression and RD (Larson et al., 2011; Spencer, 2006; Spencer et al., 2007). Among these, RD is the most prominent co-occurring condition with a prevalence rate ranging from 25% to 45% (Del'Homme et al., 2007; DuPaul et al., 2013; Willcutt & Pennington, 2000; Yoshimasu et al., 2010). However, most of the neuroimaging studies investigating neural correlates of ADHD have failed to either include a formal assessment for co-occurring RD as part of their exclusion criteria or address potential effects of co-occurring RD in their sample. The presence of comorbid RD among children with ADHD has been shown to escalate the severity of cognitive deficits commonly associated with ADHD (de Jong et al., 2009; Willcutt et al., 2010). The greater degree of severity in cognitive deficits observed in ADHD/+RD suggests exaggerated alterations in brain morphology in ADHD/+RD compared to ADHD/-RD. It is also likely that ADHD/+RD may present structural alterations in brain regions that may not be present in ADHD/-RD. Therefore, the overall goal of this dissertation research was to investigate structural alterations in brain morphology that may differentiate ADHD/+RD from ADHD/-RD and HC.

In the sample of ADHD children and adolescents recruited as part of an ongoing longitudinal study, the proportion of boys with comorbid RD was 40% (i.e. 15 out of 37),

which is at the upper end of reported prevalence values (Del'Homme et al., 2007; DuPaul et al., 2013; Willcutt & Pennington, 2000; Yoshimasu et al., 2010) and gave the unique opportunity to investigate the effects of comorbid RD in ADHD. To this end, three separate structural analyses were conducted to investigate alterations in striatal morphology, cortical thickness, and white matter integrity in boys with ADHD/-RD, ADHD/+RD and HC.

The analysis of striatal volumes showed caudate volume deficits only on the left side of ADHD/-RD compared to HC, but the effect was bilateral and to a greater degree in ADHD/+RD compared to HC (Figure 3.1). In contrast, bilateral putamen volume deficits were specific to ADHD/-RD and not present in ADHD/+RD both compared to HC (Figure 3.2). Consistent with volume results, shape analysis of striatal surface showed significant clusters reflecting inward deformation only along the left anterior and middle/posterior surface of the caudate in ADHD/-RD compared to HC (Figure 3.3), but the effect was bilateral and more widespread in ADHD/+RD compared to HC (Figure 3.4). Regarding the putamen, the surface analysis showed significant clusters reflecting inward deformations along the anterior and posterior surfaces only in ADHD/-RD relative to HC (Figure 3.5). The striatum receives projections from the frontal cortex, which are organized topographically throughout the striatum (Haber & Calzavara, 2009; Haber & Knutson, 2010). Therefore, exaggerated structural alterations in the striatum may suggest greater disturbances in the fronto-striatal networks in ADHD/+RD, which sub-serves cognitive function such as working memory, attention and cognitive control.

Unexpectedly, cortical thickness values of ADHD/-RD did not show any clusters of significant thinner cortex when compared to HC. However, ADHD/+RD showed

significant clusters of thinner cortex compared to HC in the right ACC, bilateral PC, right precuneus/posterior cingulate, right insula and Wernicke's area (Figure 4.1). Furthermore, when compared to ADHD/-RD, ADHD/+RD showed significant clusters of thinner cortex in the right ACC, Wernicke's area and left fusiform gurus (Figure 4.2). These findings suggest that ADHD/+RD present greater alterations in the regions (ACC and PC) that sub-serve attention and response inhibition along with regions (Wernicke's area and fusiform gyrus) that sub-serve orthographic processing.

Finally, in contrast to the hypothesis, DTI analysis showed no significant alterations in any of the hypothesized white matter white matter tracts. The lack of differences is plausibly due to small sample size. Therefore, future studies are warranted to investigate white matter alterations in boys with ADHD with and without comorbid RD.

Together, these finding, for the first time, provide evidence of distinctive structural alteration profile between ADHD/-RD and ADHD/+RD in striatal morphology, cortical thickness but not in white matter structure. As hypothesized, ADHD/+RD boys demonstrate exaggerated as well as additional structural alterations compared to ADHD/-RD. These differential structural alterations may underpin elevated cognitive deficits observed in ADHD/+RD. These finding provide preliminary evidence of greater disturbances in the frontostriatal and frontoparietal networks, which sub-serve executive function, attention and cognitive control. Additionally, thinner cortex observed in the Wernicke's area and fusiform gyrus provides evidence of compromised phonologic and orthographic processes respectively, which are critical for acquisition of reading skills.

As discusses in Chapter 1, the acquisition of reading skills rely on phonological processes and orthographic processes with development of phonological processes occurring first followed by development of orthographic processes (Vandermosten et al., 2012). Furthermore, attention also plays an important role in acquisition of reading skills (Semrud-Clikeman, 2012; Willcutt et al., 2005). Therefore, it can be hypothesized that the exaggerated disturbances in the attentional networks may underlie the poor development of phonologic and orthographic processes in ADHD/+RD. However, this remains to be investigated.

6.2 Implications

For the first time this study highlights the influence of comorbid RD on structural alterations among boys with ADHD. These findings will significantly impact future research and clinical practice. From a research standpoint, findings of this study are important, as it provides evidence that ADHD/+RD has a distinctive profile of structural alterations than ADHD/-RD. Most previous studies investigating structural alterations in children with ADHD have ignored the presence of comorbid RD in their sample. The finding presented in this study clearly demonstrates that ADHD/+RD should be considered as a different patient population that ADHD/-RD in future studies. Alternatively, futures studies should properly assess comorbid RD in their sample to appropriately control for the confounding effects of comorbid RD condition in their analysis. Form a clinical standpoint, the finding of this study provides support for thorough evaluation of comorbid RD condition with children with ADHD in order to determine appropriate treatment options. The standard treatment for ADHD is

psychostimulant medication along with some parent/teacher-administered behavioral therapy (Subcommittee on Attention-Deficit/Hyperactivity et al., 2011). The findings of this study clearly demonstrate that children with ADHD/+RD a distinctive pattern of morphological alterations than children with ADHD/-RD and, therefore, warrant a different therapeutic intervention than the standard recommended for ADHD.

6.3 Limitation of the Current Study

One of the limitations of the current study is the sample size, particularly after subdividing the ADHD sample into ADHD/-RD (n = 22) and ADHD/+RD (n = 15). The sample size has a significant impact on the effect size and the external validity of the study. The small sample size significantly limits the statistical power of this study. Although, the overall sample size of 66 is common in neuroimaging studies due to the cost and time needed to conduct such studies. However, the study is strengthen by utilizing additional pre-processing steps to improve and enhance the quality of data that are commonly not used in studies evaluating structural correlates of ADHD. The high-resolution T_1-weighted images were acquired in 7 separate segments and averaged offline during pre-processing. This allowed removal of segments that presented head motion resulting in T_1-weighted images that had minimal motion artifact. Similarly, the quality of DTI data was also improved by employing an automated quality control algorithm that detects and removes artifacts due to head motion and scanner hardware. Both T_1-weighted and DTI scans were further enhanced by applying an SANLM filter, which improved SNR while preserving boundary information. These quality

enhancement steps improve the accuracy of post-processing steps including registration and segmentation; thereby, increasing the validity of the findings.

Another potential limitation of the current study is the heterogeneity of the sample. Apart from comorbid RD, the ADHD sample was heterogeneous in terms of ADHD subtypes and the presence of comorbid ODD. This heterogeneity can have a confounding effect on the finding of this study. However, when the analyses were repeated by subdividing the ADHD sample based on subtypes (ADHD-combined type vs. ADHD-inattentive type) there were no significant structural differences observed between groups. Similarly, when the ADHD sample was subdivided bases on comorbid ODD, there were no significant structural differences observed between groups. These findings suggest that the heterogeneity in the sample due to ADHD subtypes and ODD did not significantly confound the findings of this study.

Finally, the current study lacks appropriate behavioral and cognitive measures to assess functional correlates of the implicated brain regions. Investigating correlations between implicated brain regions and behavioral/cognitive measures can provide insights into how structural alterations observed in this study are associated with functional outcome in these subjects. Furthermore, correlations between structural alterations and cognitive measures can confirm the hypothesis that excessive structural alterations present in ADHD/+RD are associated with greater cognitive deficits observed in these children.

6.4 Future Directions

This study demonstrates the impact of comorbid RD on the structural alterations observed in ADHD. However, the statistical power of the study is limited by the small sample size. Therefore, future studies with larger sample size are needed to validate the findings of presented in this study. Larger samples will also provide added statistical power to assess the influence ADHD subtypes and/or comorbid ODD could have on the findings of this study. The study clearly shows a distinct pattern of structural alterations between ADHD/-RD and ADHD/+RD. This raises an important question: does ADHD/-RD have a different developmental profile than ADHD/+RD. Longitudinal studies are needed to address this question. Finally, future studies can enhance the findings and conclusions of this study by evaluating cognitive and behavioral correlates associated with structural differences between ADHD/-RD and ADHD/+RD.

REFERENCES

Alexander, A. L., Lee, J. E., Lazar, M., & Field, A. S. (2007). Diffusion tensor imaging of the brain. *Neurotherapeutics, 4*(3), 316-329. doi: 10.1016/j.nurt.2007.05.011

Almeida, L. G., Ricardo-Garcell, J., Prado, H., Barajas, L., Fernandez-Bouzas, A., Avila, D., & Martinez, R. B. (2010). Reduced right frontal cortical thickness in children, adolescents and adults with ADHD and its correlation to clinical variables: a cross-sectional study. *J Psychiatr Res, 44*(16), 1214-1223. doi: 10.1016/j.jpsychires.2010.04.026

Almeida Montes, L. G., Prado Alcantara, H., Martinez Garcia, R. B., De La Torre, L. B., Avila Acosta, D., & Duarte, M. G. (2013). Brain cortical thickness in ADHD: age, sex, and clinical correlations. *J Atten Disord, 17*(8), 641-654. doi: 10.1177/1087054711434351

American Psychiatric Association. (2000). *Diagnostic criteria from DSM-IV-TR*. Washington, D.C.: American Psychiatric Association.

American Psychiatric Association. (2013). *Diagnostic and statistical manual of mental disorders : DSM-5* (5th ed.). Washington, D.C.: American Psychiatric Association.

Arnsten, A. F., & Rubia, K. (2012). Neurobiological circuits regulating attention, cognitive control, motivation, and emotion: disruptions in neurodevelopmental psychiatric disorders. *J Am Acad Child Adolesc Psychiatry, 51*(4), 356-367. doi: 10.1016/j.jaac.2012.01.008

Ashtari, M., Kumra, S., Bhaskar, S. L., Clarke, T., Thaden, E., Cervellione, K. L., . . . Ardekani, B. A. (2005). Attention-deficit/hyperactivity disorder: a preliminary

diffusion tensor imaging study. *Biol Psychiatry, 57*(5), 448-455. doi: 10.1016/j.biopsych.2004.11.047

Banerjee, T. D., Middleton, F., & Faraone, S. V. (2007). Environmental risk factors for attention-deficit hyperactivity disorder. *Acta Paediatr, 96*(9), 1269-1274. doi: 10.1111/j.1651-2227.2007.00430.x

Barkley, R. A. (1997). Behavioral inhibition, sustained attention, and executive functions: constructing a unifying theory of ADHD. *Psychol Bull, 121*(1), 65-94.

Basser, P. J., Mattiello, J., & LeBihan, D. (1994). Estimation of the effective self-diffusion tensor from the NMR spin echo. *J Magn Reson B, 103*(3), 247-254.

Batty, M. J., Liddle, E. B., Pitiot, A., Toro, R., Groom, M. J., Scerif, G., . . . Hollis, C. (2010). Cortical gray matter in attention-deficit/hyperactivity disorder: a structural magnetic resonance imaging study. *J Am Acad Child Adolesc Psychiatry, 49*(3), 229-238.

Behrens, T. E., Woolrich, M. W., Jenkinson, M., Johansen-Berg, H., Nunes, R. G., Clare, S., . . . Smith, S. M. (2003). Characterization and propagation of uncertainty in diffusion-weighted MR imaging. *Magn Reson Med, 50*(5), 1077-1088. doi: 10.1002/mrm.10609

Brown, M. A., & Semelka, R. C. (2010). *MRI : basic principles and applications* (4th ed.). Hoboken, N.J.: Wiley-Blackwell/John Wiley & Sons.

Buckner, R. L., Head, D., Parker, J., Fotenos, A. F., Marcus, D., Morris, J. C., & Snyder, A. Z. (2004). A unified approach for morphometric and functional data analysis in young, old, and demented adults using automated atlas-based head size normalization: reliability and validation against manual measurement of total

intracranial volume. *Neuroimage, 23*(2), 724-738. doi: 10.1016/j.neuroimage.2004.06.018

Bush, G. (2011). Cingulate, frontal, and parietal cortical dysfunction in attention-deficit/hyperactivity disorder. *Biol Psychiatry, 69*(12), 1160-1167. doi: 10.1016/j.biopsych.2011.01.022

Canu, E., McLaren, D. G., Fitzgerald, M. E., Bendlin, B. B., Zoccatelli, G., Alessandrini, F., . . . Frisoni, G. B. (2010). Microstructural diffusion changes are independent of macrostructural volume loss in moderate to severe Alzheimer's disease. *J Alzheimers Dis, 19*(3), 963-976. doi: 10.3233/JAD-2010-1295

Carter, J. C., Lanham, D. C., Cutting, L. E., Clements-Stephens, A. M., Chen, X., Hadzipasic, M., . . . Kaufmann, W. E. (2009). A dual DTI approach to analyzing white matter in children with dyslexia. *Psychiatry Res, 172*(3), 215-219. doi: 10.1016/j.pscychresns.2008.09.005

Castellanos, F. X., Giedd, J. N., Berquin, P. C., Walter, J. M., Sharp, W., Tran, T., . . . Rapoport, J. L. (2001). Quantitative brain magnetic resonance imaging in girls with attention-deficit/hyperactivity disorder. *Arch Gen Psychiatry, 58*(3), 289-295.

Castellanos, F. X., Giedd, J. N., Marsh, W. L., Hamburger, S. D., Vaituzis, A. C., Dickstein, D. P., . . . Rapoport, J. L. (1996). Quantitative brain magnetic resonance imaging in attention-deficit hyperactivity disorder. *Arch Gen Psychiatry, 53*(7), 607-616.

Castellanos, F. X., Lee, P. P., Sharp, W., Jeffries, N. O., Greenstein, D. K., Clasen, L. S., . . . Rapoport, J. L. (2002). Developmental trajectories of brain volume

abnormalities in children and adolescents with attention-deficit/hyperactivity disorder. *JAMA, 288*(14), 1740-1748.

Chumbley, J. R., & Friston, K. J. (2009). False discovery rate revisited: FDR and topological inference using Gaussian random fields. *Neuroimage, 44*(1), 62-70. doi: 10.1016/j.neuroimage.2008.05.021

Chumbley, J. R., Worsley, K., Flandin, G., & Friston, K. (2010). Topological FDR for neuroimaging. *Neuroimage, 49*(4), 3057-3064. doi: 10.1016/j.neuroimage.2009.10.090

Cone, N. E., Burman, D. D., Bitan, T., Bolger, D. J., & Booth, J. R. (2008). Developmental changes in brain regions involved in phonological and orthographic processing during spoken language processing. *Neuroimage, 41*(2), 623-635. doi: 10.1016/j.neuroimage.2008.02.055

Currie, J., & Stabile, M. (2006). Child mental health and human capital accumulation: the case of ADHD. *J Health Econ, 25*(6), 1094-1118. doi: 10.1016/j.jhealeco.2006.03.001

Dale, A. M., Fischl, B., & Sereno, M. I. (1999). Cortical surface-based analysis. I. Segmentation and surface reconstruction. *Neuroimage, 9*(2), 179-194.

Dale, A. M., & Sereno, M. I. (1993). Improved localization of cortical activity by combining EEG and MEG with MRI cortical surface reconstruction: a linear approach. *J Cogn Neurosci, 5*, 162-176.

Davenport, N. D., Karatekin, C., White, T., & Lim, K. O. (2010). Differential fractional anisotropy abnormalities in adolescents with ADHD or schizophrenia. *Psychiatry Res, 181*(3), 193-198. doi: 10.1016/j.pscychresns.2009.10.012

De Graaf, R. A. (2013). *In vivo NMR spectroscopy: principles and techniques*: John Wiley & Sons.

de Jong, C. G., Van De Voorde, S., Roeyers, H., Raymaekers, R., Oosterlaan, J., & Sergeant, J. A. (2009). How distinctive are ADHD and RD? Results of a double dissociation study. *J Abnorm Child Psychol, 37*(7), 1007-1017. doi: 10.1007/s10802-009-9328-y

Del'Homme, M., Kim, T. S., Loo, S. K., Yang, M. H., & Smalley, S. L. (2007). Familial association and frequency of learning disabilities in ADHD sibling pair families. *J Abnorm Child Psychol, 35*(1), 55-62. doi: 10.1007/s10802-006-9080-5

Derks, E. M., Dolan, C. V., Hudziak, J. J., Neale, M. C., & Boomsma, D. I. (2007). Assessment and etiology of attention deficit hyperactivity disorder and oppositional defiant disorder in boys and girls. *Behav Genet, 37*(4), 559-566. doi: 10.1007/s10519-007-9153-4

Desikan, R. S., Segonne, F., Fischl, B., Quinn, B. T., Dickerson, B. C., Blacker, D., . . . Killiany, R. J. (2006). An automated labeling system for subdividing the human cerebral cortex on MRI scans into gyral based regions of interest. *Neuroimage, 31*(3), 968-980.

Draganski, B., Kherif, F., Kloppel, S., Cook, P. A., Alexander, D. C., Parker, G. J., . . . Frackowiak, R. S. (2008). Evidence for segregated and integrative connectivity patterns in the human Basal Ganglia. *J Neurosci, 28*(28), 7143-7152. doi: 10.1523/JNEUROSCI.1486-08.2008

DuPaul, G. J., Gormley, M. J., & Laracy, S. D. (2013). Comorbidity of LD and ADHD: implications of DSM-5 for assessment and treatment. *J Learn Disabil, 46*(1), 43-51. doi: 10.1177/0022219412464351

Durston, S., Hulshoff Pol, H. E., Schnack, H. G., Buitelaar, J. K., Steenhuis, M. P., Minderaa, R. B., . . . van Engeland, H. (2004). Magnetic resonance imaging of boys with attention-deficit/hyperactivity disorder and their unaffected siblings. *J Am Acad Child Adolesc Psychiatry, 43*(3), 332-340.

Faraone, S. V., Biederman, J., & Mick, E. (2006). The age-dependent decline of attention deficit hyperactivity disorder: a meta-analysis of follow-up studies. *Psychol Med, 36*(2), 159-165. doi: 10.1017/S003329170500471X

Faraone, S. V., Biederman, J., Weber, W., & Russell, R. L. (1998). Psychiatric, neuropsychological, and psychosocial features of DSM-IV subtypes of attention-deficit/hyperactivity disorder: results from a clinically referred sample. *J Am Acad Child Adolesc Psychiatry, 37*(2), 185-193. doi: 10.1097/00004583-199802000-00011

Faraone, S. V., Sergeant, J., Gillberg, C., & Biederman, J. (2003). The worldwide prevalence of ADHD: is it an American condition? *World Psychiatry, 2*(2), 104-113.

Fischl, B., & Dale, A. M. (2000). Measuring the thickness of the human cerebral cortex from magnetic resonance images. *Proc Natl Acad Sci U S A, 97*(20), 11050-11055.

Fischl, B., Liu, A., & Dale, A. M. (2001). Automated manifold surgery: constructing geometrically accurate and topologically correct models of the human cerebral cortex. *IEEE Trans Med Imaging, 20*(1), 70-80.

Fischl, B., Salat, D. H., Busa, E., Albert, M., Dieterich, M., Haselgrove, C., . . . Dale, A. M. (2002). Whole brain segmentation: automated labeling of neuroanatomical structures in the human brain. *Neuron, 33*(3), 341-355.

Fischl, B., Salat, D. H., van der Kouwe, A. J., Makris, N., Segonne, F., Quinn, B. T., & Dale, A. M. (2004). Sequence-independent segmentation of magnetic resonance images. *Neuroimage, 23 Suppl 1*, S69-84.

Fischl, B., Sereno, M. I., & Dale, A. M. (1999). Cortical surface-based analysis. II: Inflation, flattening, and a surface-based coordinate system. *Neuroimage, 9*(2), 195-207.

Fischl, B., Sereno, M. I., Tootell, R. B., & Dale, A. M. (1999). High-resolution intersubject averaging and a coordinate system for the cortical surface. *Hum Brain Mapp, 8*(4), 272-284.

Fischl, B., van der Kouwe, A., Destrieux, C., Halgren, E., Segonne, F., Salat, D. H., . . . Dale, A. M. (2004). Automatically parcellating the human cerebral cortex. *Cereb Cortex, 14*(1), 11-22.

Fjell, A. M., Westlye, L. T., Greve, D. N., Fischl, B., Benner, T., van der Kouwe, A. J., . . . Walhovd, K. B. (2008). The relationship between diffusion tensor imaging and volumetry as measures of white matter properties. *Neuroimage, 42*(4), 1654-1668. doi: 10.1016/j.neuroimage.2008.06.005

Fonov, V., Evans, A. C., Botteron, K., Almli, C. R., McKinstry, R. C., Collins, D. L., & Brain Development Cooperative, G. (2011). Unbiased average age-appropriate atlases for pediatric studies. *Neuroimage, 54*(1), 313-327. doi: 10.1016/j.neuroimage.2010.07.033

Friedman, L. A., & Rapoport, J. L. (2015). Brain development in ADHD. *Curr Opin Neurobiol, 30*, 106-111. doi: 10.1016/j.conb.2014.11.007

Germano, E., Gagliano, A., & Curatolo, P. (2010). Comorbidity of ADHD and dyslexia. *Dev Neuropsychol, 35*(5), 475-493. doi: 10.1080/87565641.2010.494748

Haber, S. N., & Calzavara, R. (2009). The cortico-basal ganglia integrative network: the role of the thalamus. *Brain Res Bull, 78*(2-3), 69-74. doi: 10.1016/j.brainresbull.2008.09.013

Haber, S. N., & Knutson, B. (2010). The reward circuit: linking primate anatomy and human imaging. *Neuropsychopharmacology, 35*(1), 4-26. doi: 10.1038/npp.2009.129

Han, X., Jovicich, J., Salat, D., van der Kouwe, A., Quinn, B., Czanner, S., . . . Fischl, B. (2006). Reliability of MRI-derived measurements of human cerebral cortical thickness: the effects of field strength, scanner upgrade and manufacturer. *Neuroimage, 32*(1), 180-194.

Hawke, J. L., Wadsworth, S. J., Olson, R. K., & DeFries, J. C. (2007). Etiology of reading difficulties as a function of gender and severity. *Reading and Writing, 20*, 13-25.

Hoekzema, E., Carmona, S., Ramos-Quiroga, J. A., Richarte Fernandez, V., Picado, M., Bosch, R., . . . Vilarroya, O. (2012). Laminar thickness alterations in the

fronto-parietal cortical mantle of patients with attention-deficit/hyperactivity disorder. *PLoS One, 7*(12), e48286. doi: 10.1371/journal.pone.0048286

Hugenschmidt, C. E., Peiffer, A. M., Kraft, R. A., Casanova, R., Deibler, A. R., Burdette, J. H., . . . Laurienti, P. J. (2008). Relating imaging indices of white matter integrity and volume in healthy older adults. *Cereb Cortex, 18*(2), 433-442. doi: 10.1093/cercor/bhm080

Hutton, C., Draganski, B., Ashburner, J., & Weiskopf, N. (2009). A comparison between voxel-based cortical thickness and voxel-based morphometry in normal aging. *Neuroimage, 48*(2), 371-380. doi: 10.1016/j.neuroimage.2009.06.043

Jenkinson, M., Bannister, P., Brady, M., & Smith, S. (2002). Improved optimization for the robust and accurate linear registration and motion correction of brain images. *Neuroimage, 17*(2), 825-841.

Jenkinson, M., & Smith, S. (2001). A global optimisation method for robust affine registration of brain images. *Med Image Anal, 5*(2), 143-156.

Jones, D. K., & Cercignani, M. (2010). Twenty-five pitfalls in the analysis of diffusion MRI data. *NMR Biomed, 23*(7), 803-820. doi: 10.1002/nbm.1543

Jovicich, J., Czanner, S., Greve, D., Haley, E., van der Kouwe, A., Gollub, R., . . . Dale, A. (2006). Reliability in multi-site structural MRI studies: effects of gradient non-linearity correction on phantom and human data. *Neuroimage, 30*(2), 436-443.

Kates, W. R., Frederikse, M., Mostofsky, S. H., Folley, B. S., Cooper, K., Mazur-Hopkins, P., . . . Kaufmann, W. E. (2002). MRI parcellation of the frontal lobe in boys with attention deficit hyperactivity disorder or Tourette syndrome. *Psychiatry Res, 116*(1-2), 63-81.

Kaufman, J., Birmaher, B., Brent, D., Rao, U., Flynn, C., Moreci, P., . . . Ryan, N. (1997). Schedule for Affective Disorders and Schizophrenia for School-Age Children-Present and Lifetime Version (K-SADS-PL): initial reliability and validity data. *J Am Acad Child Adolesc Psychiatry, 36*(7), 980-988. doi: 10.1097/00004583-199707000-00021

Kobel, M., Bechtel, N., Specht, K., Klarhofer, M., Weber, P., Scheffler, K., . . . Penner, I. K. (2010). Structural and functional imaging approaches in attention deficit/hyperactivity disorder: does the temporal lobe play a key role? *Psychiatry Res, 183*(3), 230-236. doi: 10.1016/j.pscychresns.2010.03.010

Kochunov, P., Lancaster, J. L., Glahn, D. C., Purdy, D., Laird, A. R., Gao, F., & Fox, P. (2006). Retrospective motion correction protocol for high-resolution anatomical MRI. *Hum Brain Mapp, 27*(12), 957-962. doi: 10.1002/hbm.20235

Konrad, A., Dielentheis, T. F., El Masri, D., Bayerl, M., Fehr, C., Gesierich, T., . . . Winterer, G. (2010). Disturbed structural connectivity is related to inattention and impulsivity in adult attention deficit hyperactivity disorder. *Eur J Neurosci, 31*(5), 912-919. doi: 10.1111/j.1460-9568.2010.07110.x

Krain, A. L., & Castellanos, F. X. (2006). Brain development and ADHD. *Clin Psychol Rev, 26*(4), 433-444. doi: 10.1016/j.cpr.2006.01.005

Kuperberg, G. R., Broome, M. R., McGuire, P. K., David, A. S., Eddy, M., Ozawa, F., . . . Fischl, B. (2003). Regionally localized thinning of the cerebral cortex in schizophrenia. *Arch Gen Psychiatry, 60*(9), 878-888.

Lacerda, A. L., Nicoletti, M. A., Brambilla, P., Sassi, R. B., Mallinger, A. G., Frank, E., . . . Soares, J. C. (2003). Anatomical MRI study of basal ganglia in major depressive disorder. *Psychiatry Res, 124*(3), 129-140.

Lahey, B. B., Applegate, B., McBurnett, K., Biederman, J., Greenhill, L., Hynd, G. W., . . . et al. (1994). DSM-IV field trials for attention deficit hyperactivity disorder in children and adolescents. *Am J Psychiatry, 151*(11), 1673-1685.

Larson, K., Russ, S. A., Kahn, R. S., & Halfon, N. (2011). Patterns of comorbidity, functioning, and service use for US children with ADHD, 2007. *Pediatrics, 127*(3), 462-470. doi: 10.1542/peds.2010-0165

Le Bihan, D., Mangin, J. F., Poupon, C., Clark, C. A., Pappata, S., Molko, N., & Chabriat, H. (2001). Diffusion tensor imaging: concepts and applications. *J Magn Reson Imaging, 13*(4), 534-546.

Leemans, A., & Jones, D. K. (2009). The B-matrix must be rotated when correcting for subject motion in DTI data. *Magn Reson Med, 61*(6), 1336-1349. doi: 10.1002/mrm.21890

Leh, S. E., Ptito, A., Chakravarty, M. M., & Strafella, A. P. (2007). Fronto-striatal connections in the human brain: a probabilistic diffusion tractography study. *Neurosci Lett, 419*(2), 113-118. doi: 10.1016/j.neulet.2007.04.049

Lehericy, S., Ducros, M., Van de Moortele, P. F., Francois, C., Thivard, L., Poupon, C., . . . Kim, D. S. (2004). Diffusion tensor fiber tracking shows distinct corticostriatal circuits in humans. *Ann Neurol, 55*(4), 522-529. doi: 10.1002/ana.20030

Li, Q., Sun, J., Guo, L., Zang, Y., Feng, Z., Huang, X., . . . Gong, Q. (2010). Increased fractional anisotropy in white matter of the right frontal region in children with

attention-deficit/hyperactivity disorder: a diffusion tensor imaging study. *Neuro Endocrinol Lett, 31*(6), 747-753.

Ling, J., Merideth, F., Caprihan, A., Pena, A., Teshiba, T., & Mayer, A. R. (2012). Head injury or head motion? Assessment and quantification of motion artifacts in diffusion tensor imaging studies. *Hum Brain Mapp, 33*(1), 50-62. doi: 10.1002/hbm.21192

Liu, Z., Wang, Y., Gerig, G., Gouttard, S., Tao, R., Fletcher, T., & Styner, M. (2010). Quality Control of Diffusion Weighted Images. *Proc SPIE Int Soc Opt Eng, 7628*. doi: 10.1117/12.844748

Loney, J., & Milich, R. (1982). Hyperactivity, Inattention and Aggression in Clinical Practice. In M. Wolraich (Ed.), *Advances in Developmental and Behavioral Pediatrics.* (Vol. 3, pp. 113-147). Greenwich, Conn: JAI Press.

Manjon, J. V., Coupe, P., Marti-Bonmati, L., Collins, D. L., & Robles, M. (2010). Adaptive non-local means denoising of MR images with spatially varying noise levels. *J Magn Reson Imaging, 31*(1), 192-203. doi: 10.1002/jmri.22003

Maughan, B., & Carroll, J. (2006). Literacy and mental disorders. *Curr Opin Psychiatry, 19*(4), 350-354. doi: 10.1097/01.yco.0000228752.79990.41

McAlonan, G. M., Cheung, V., Cheung, C., Chua, S. E., Murphy, D. G., Suckling, J., . . . Ho, T. P. (2007). Mapping brain structure in attention deficit-hyperactivity disorder: a voxel-based MRI study of regional grey and white matter volume. *Psychiatry Res, 154*(2), 171-180. doi: 10.1016/j.pscychresns.2006.09.006

Nagel, B. J., Bathula, D., Herting, M., Schmitt, C., Kroenke, C. D., Fair, D., & Nigg, J. T. (2011). Altered white matter microstructure in children with attention-

deficit/hyperactivity disorder. *J Am Acad Child Adolesc Psychiatry, 50*(3), 283-292. doi: 10.1016/j.jaac.2010.12.003

Narr, K. L., Woods, R. P., Lin, J., Kim, J., Phillips, O. R., Del'Homme, M., . . . Levitt, J. G. (2009). Widespread cortical thinning is a robust anatomical marker for attention-deficit/hyperactivity disorder. *J Am Acad Child Adolesc Psychiatry, 48*(10), 1014-1022. doi: 10.1097/CHI.0b013e3181b395c0

Nigg, J. T. (2013). Attention deficits and hyperactivity-impulsivity: what have we learned, what next? *Dev Psychopathol, 25*(4 Pt 2), 1489-1503. doi: 10.1017/S0954579413000734

Nigg, J. T., & Casey, B. J. (2005). An integrative theory of attention-deficit/ hyperactivity disorder based on the cognitive and affective neurosciences. *Dev Psychopathol, 17*(3), 785-806. doi: 10.1017/S0954579405050376

Norton, E. S., Beach, S. D., & Gabrieli, J. D. (2015). Neurobiology of dyslexia. *Curr Opin Neurobiol, 30*, 73-78. doi: 10.1016/j.conb.2014.09.007

Oguz, I., Farzinfar, M., Matsui, J., Budin, F., Liu, Z., Gerig, G., . . . Styner, M. (2014). DTIPrep: quality control of diffusion-weighted images. *Front Neuroinform, 8*, 4. doi: 10.3389/fninf.2014.00004

Olson, R. K. (2002). Dyslexia: nature and nurture. *Dyslexia, 8*(3), 143-159. doi: 10.1002/dys.228

Pastor, P. N., & Reuben, C. A. (2008). Diagnosed attention deficit hyperactivity disorder and learning disability: United States, 2004-2006. *Vital Health Stat 10*(237), 1-14.

Patenaude, B., Smith, S. M., Kennedy, D. N., & Jenkinson, M. (2011). A Bayesian model of shape and appearance for subcortical brain segmentation. *Neuroimage, 56*(3), 907-922. doi: 10.1016/j.neuroimage.2011.02.046

Pelham, W. E., Foster, E. M., & Robb, J. A. (2007). The economic impact of attention-deficit/hyperactivity disorder in children and adolescents. *J Pediatr Psychol, 32*(6), 711-727. doi: 10.1093/jpepsy/jsm022

Pelham, W. E., Jr., Gnagy, E. M., Greenslade, K. E., & Milich, R. (1992). Teacher ratings of DSM-III-R symptoms for the disruptive behavior disorders. *J Am Acad Child Adolesc Psychiatry, 31*(2), 210-218. doi: 10.1097/00004583-199203000-00006

Peterson, D. J., Ryan, M., Rimrodt, S. L., Cutting, L. E., Denckla, M. B., Kaufmann, W. E., & Mahone, E. M. (2011). Increased regional fractional anisotropy in highly screened attention-deficit hyperactivity disorder (ADHD). *J Child Neurol, 26*(10), 1296-1302. doi: 10.1177/0883073811405662

Polanczyk, G., de Lima, M. S., Horta, B. L., Biederman, J., & Rohde, L. A. (2007). The worldwide prevalence of ADHD: a systematic review and metaregression analysis. *Am J Psychiatry, 164*(6), 942-948. doi: 10.1176/ajp.2007.164.6.942

Polanczyk, G. V., Willcutt, E. G., Salum, G. A., Kieling, C., & Rohde, L. A. (2014). ADHD prevalence estimates across three decades: an updated systematic review and meta-regression analysis. *Int J Epidemiol, 43*(2), 434-442. doi: 10.1093/ije/dyt261

Psychological Corporation. (2009). WIAT III Wechsler Individual Achievement Test.

Qiu, A., Crocetti, D., Adler, M., Mahone, E. M., Denckla, M. B., Miller, M. I., & Mostofsky, S. H. (2009). Basal ganglia volume and shape in children with

attention deficit hyperactivity disorder. *Am J Psychiatry, 166*(1), 74-82. doi: 10.1176/appi.ajp.2008.08030426

Qiu, M. G., Ye, Z., Li, Q. Y., Liu, G. J., Xie, B., & Wang, J. (2011). Changes of brain structure and function in ADHD children. *Brain Topogr, 24*(3-4), 243-252. doi: 10.1007/s10548-010-0168-4

Rimrodt, S. L., Peterson, D. J., Denckla, M. B., Kaufmann, W. E., & Cutting, L. E. (2010). White matter microstructural differences linked to left perisylvian language network in children with dyslexia. *Cortex, 46*(6), 739-749. doi: 10.1016/j.cortex.2009.07.008

Rohde, L. A., Biederman, J., Busnello, E. A., Zimmermann, H., Schmitz, M., Martins, S., & Tramontina, S. (1999). ADHD in a school sample of Brazilian adolescents: a study of prevalence, comorbid conditions, and impairments. *J Am Acad Child Adolesc Psychiatry, 38*(6), 716-722. doi: 10.1097/00004583-199906000-00019

Rosas, H. D., Liu, A. K., Hersch, S., Glessner, M., Ferrante, R. J., Salat, D. H., . . . Fischl, B. (2002). Regional and progressive thinning of the cortical ribbon in Huntington's disease. *Neurology, 58*(5), 695-701.

Rutter, M., Caspi, A., Fergusson, D., Horwood, L. J., Goodman, R., Maughan, B., . . . Carroll, J. (2004). Sex differences in developmental reading disability: new findings from 4 epidemiological studies. *JAMA, 291*(16), 2007-2012. doi: 10.1001/jama.291.16.2007

Sanches, M., Roberts, R. L., Sassi, R. B., Axelson, D., Nicoletti, M., Brambilla, P., . . . Soares, J. C. (2005). Developmental abnormalities in striatum in young bipolar

patients: a preliminary study. *Bipolar Disord, 7*(2), 153-158. doi: 10.1111/j.1399-5618.2004.00178.x

Schneider, J. F., Il'yasov, K. A., Boltshauser, E., Hennig, J., & Martin, E. (2003). Diffusion tensor imaging in cases of adrenoleukodystrophy: preliminary experience as a marker for early demyelination? *AJNR Am J Neuroradiol, 24*(5), 819-824.

Segonne, F., Dale, A. M., Busa, E., Glessner, M., Salat, D., Hahn, H. K., & Fischl, B. (2004). A hybrid approach to the skull stripping problem in MRI. *Neuroimage, 22*(3), 1060-1075.

Semrud-Clikeman, M. (2012). The role of inattention on academics, fluid reasoning, and visual-spatial functioning in two subtypes of ADHD. *Appl Neuropsychol Child, 1*(1), 18-29. doi: 10.1080/21622965.2012.665766

Semrud-Clikeman, M., Pliszka, S. R., Lancaster, J., & Liotti, M. (2006). Volumetric MRI differences in treatment-naive vs chronically treated children with ADHD. *Neurology, 67*(6), 1023-1027. doi: 10.1212/01.wnl.0000237385.84037.3c

Sexton, C. C., Gelhorn, H. L., Bell, J. A., & Classi, P. M. (2012). The co-occurrence of reading disorder and ADHD: epidemiology, treatment, psychosocial impact, and economic burden. *J Learn Disabil, 45*(6), 538-564. doi: 10.1177/0022219411407772

Shaffer, D., Could, M. S., Brasic, J., Ambrosini, P., Fisher, P., Bird, H., & Aluwahlia, S. (1983). A children's global assessment scale (CGAS). *Arch Gen Psychiatry, 40*(11), 1228-1231. doi: 10.1001/archpsyc.1983.01790100074010

Shaw, P., De Rossi, P., Watson, B., Wharton, A., Greenstein, D., Raznahan, A., . . . Chakravarty, M. M. (2014). Mapping the development of the basal ganglia in children with attention-deficit/hyperactivity disorder. *J Am Acad Child Adolesc Psychiatry, 53*(7), 780-789 e711. doi: 10.1016/j.jaac.2014.05.003

Shaw, P., Eckstrand, K., Sharp, W., Blumenthal, J., Lerch, J. P., Greenstein, D., . . . Rapoport, J. L. (2007). Attention-deficit/hyperactivity disorder is characterized by a delay in cortical maturation. *Proc Natl Acad Sci U S A, 104*(49), 19649-19654. doi: 10.1073/pnas.0707741104

Shaw, P., Lalonde, F., Lepage, C., Rabin, C., Eckstrand, K., Sharp, W., . . . Rapoport, J. (2009). Development of cortical asymmetry in typically developing children and its disruption in attention-deficit/hyperactivity disorder. *Arch Gen Psychiatry, 66*(8), 888-896. doi: 10.1001/archgenpsychiatry.2009.103

Shaw, P., Lerch, J., Greenstein, D., Sharp, W., Clasen, L., Evans, A., . . . Rapoport, J. (2006). Longitudinal mapping of cortical thickness and clinical outcome in children and adolescents with attention-deficit/hyperactivity disorder. *Arch Gen Psychiatry, 63*(5), 540-549. doi: 10.1001/archpsyc.63.5.540

Shaw, P., & Rabin, C. (2009). New insights into attention-deficit/hyperactivity disorder using structural neuroimaging. *Curr Psychiatry Rep, 11*(5), 393-398.

Silk, T. J., Vance, A., Rinehart, N., Bradshaw, J. L., & Cunnington, R. (2009). White-matter abnormalities in attention deficit hyperactivity disorder: a diffusion tensor imaging study. *Hum Brain Mapp, 30*(9), 2757-2765. doi: 10.1002/hbm.20703

Sled, J. G., Zijdenbos, A. P., & Evans, A. C. (1998). A nonparametric method for automatic correction of intensity nonuniformity in MRI data. *IEEE Trans Med Imaging, 17*(1), 87-97.

Smith, S. M. (2002). Fast robust automated brain extraction. *Hum Brain Mapp, 17*(3), 143-155. doi: 10.1002/hbm.10062

Sobel, L. J., Bansal, R., Maia, T. V., Sanchez, J., Mazzone, L., Durkin, K., . . . Peterson, B. S. (2010). Basal ganglia surface morphology and the effects of stimulant medications in youth with attention deficit hyperactivity disorder. *Am J Psychiatry, 167*(8), 977-986. doi: 10.1176/appi.ajp.2010.09091259

Song, S. K., Sun, S. W., Ju, W. K., Lin, S. J., Cross, A. H., & Neufeld, A. H. (2003). Diffusion tensor imaging detects and differentiates axon and myelin degeneration in mouse optic nerve after retinal ischemia. *Neuroimage, 20*(3), 1714-1722.

Song, S. K., Sun, S. W., Ramsbottom, M. J., Chang, C., Russell, J., & Cross, A. H. (2002). Dysmyelination revealed through MRI as increased radial (but unchanged axial) diffusion of water. *Neuroimage, 17*(3), 1429-1436.

Sonuga-Barke, E. J. (2005). Causal models of attention-deficit/hyperactivity disorder: from common simple deficits to multiple developmental pathways. *Biol Psychiatry, 57*(11), 1231-1238. doi: 10.1016/j.biopsych.2004.09.008

Spencer, T. J. (2006). ADHD and comorbidity in childhood. *J Clin Psychiatry, 67 Suppl 8*, 27-31.

Spencer, T. J., Biederman, J., & Mick, E. (2007). Attention-deficit/hyperactivity disorder: diagnosis, lifespan, comorbidities, and neurobiology. *J Pediatr Psychol, 32*(6), 631-642. doi: 10.1093/jpepsy/jsm005

Steinbrink, C., Vogt, K., Kastrup, A., Muller, H. P., Juengling, F. D., Kassubek, J., & Riecker, A. (2008). The contribution of white and gray matter differences to developmental dyslexia: insights from DTI and VBM at 3.0 T. *Neuropsychologia, 46*(13), 3170-3178. doi: 10.1016/j.neuropsychologia.2008.07.015

Strine, T. W., Lesesne, C. A., Okoro, C. A., McGuire, L. C., Chapman, D. P., Balluz, L. S., & Mokdad, A. H. (2006). Emotional and behavioral difficulties and impairments in everyday functioning among children with a history of attention-deficit/hyperactivity disorder. *Prev Chronic Dis, 3*(2), A52.

Styner, M., Oguz, I., Xu, S., Brechbuhler, C., Pantazis, D., Levitt, J. J., . . . Gerig, G. (2006). Framework for the Statistical Shape Analysis of Brain Structures using SPHARM-PDM. *Insight J*(1071), 242-250.

Subcommittee on Attention-Deficit/Hyperactivity, D., Steering Committee on Quality, I., Management, Wolraich, M., Brown, L., Brown, R. T., . . . Visser, S. (2011). ADHD: clinical practice guideline for the diagnosis, evaluation, and treatment of attention-deficit/hyperactivity disorder in children and adolescents. *Pediatrics, 128*(5), 1007-1022. doi: 10.1542/peds.2011-2654

Sun, Y. F., Lee, J. S., & Kirby, R. (2010). Brain imaging findings in dyslexia. *Pediatr Neonatol, 51*(2), 89-96. doi: 10.1016/S1875-9572(10)60017-4

Suzuki, Y., Matsuzawa, H., Kwee, I. L., & Nakada, T. (2003). Absolute eigenvalue diffusion tensor analysis for human brain maturation. *NMR Biomed, 16*(5), 257-260. doi: 10.1002/nbm.848

Thomas, R., Sanders, S., Doust, J., Beller, E., & Glasziou, P. (2015). Prevalence of Attention-Deficit/Hyperactivity Disorder: A Systematic Review and Meta-analysis. *Pediatrics*. doi: 10.1542/peds.2014-3482

Tremols, V., Bielsa, A., Soliva, J. C., Raheb, C., Carmona, S., Tomas, J., . . . Vilarroya, O. (2008). Differential abnormalities of the head and body of the caudate nucleus in attention deficit-hyperactivity disorder. *Psychiatry Res, 163*(3), 270-278. doi: 10.1016/j.pscychresns.2007.04.017

Ullman, M. T. (2006). Is Broca's area part of a basal ganglia thalamocortical circuit? *Cortex, 42*(4), 480-485.

Valera, E. M., Faraone, S. V., Murray, K. E., & Seidman, L. J. (2007). Meta-analysis of structural imaging findings in attention-deficit/hyperactivity disorder. *Biol Psychiatry, 61*(12), 1361-1369. doi: 10.1016/j.biopsych.2006.06.011

van Ewijk, H., Heslenfeld, D. J., Zwiers, M. P., Buitelaar, J. K., & Oosterlaan, J. (2012). Diffusion tensor imaging in attention deficit/hyperactivity disorder: a systematic review and meta-analysis. *Neurosci Biobehav Rev, 36*(4), 1093-1106. doi: 10.1016/j.neubiorev.2012.01.003

Vandermosten, M., Boets, B., Poelmans, H., Sunaert, S., Wouters, J., & Ghesquiere, P. (2012). A tractography study in dyslexia: neuroanatomic correlates of orthographic, phonological and speech processing. *Brain, 135*(Pt 3), 935-948. doi: 10.1093/brain/awr363

Vogel, S. A. (1990). Gender differences in intelligence, language, visual-motor abilities, and academic achievement in students with learning disabilities: a review of the literature. *J Learn Disabil, 23*(1), 44-52.

Wechsler, D. (1999). *Wechsler abbreviated scale of intelligence WASI : manual*. San Antonio: Pearson/PsychCorpl.

Willcutt, E. G. (2012). The prevalence of DSM-IV attention-deficit/hyperactivity disorder: a meta-analytic review. *Neurotherapeutics, 9*(3), 490-499. doi: 10.1007/s13311-012-0135-8

Willcutt, E. G., Betjemann, R. S., McGrath, L. M., Chhabildas, N. A., Olson, R. K., DeFries, J. C., & Pennington, B. F. (2010). Etiology and neuropsychology of comorbidity between RD and ADHD: the case for multiple-deficit models. *Cortex, 46*(10), 1345-1361. doi: 10.1016/j.cortex.2010.06.009

Willcutt, E. G., & Pennington, B. F. (2000). Comorbidity of reading disability and attention-deficit/hyperactivity disorder: differences by gender and subtype. *J Learn Disabil, 33*(2), 179-191.

Willcutt, E. G., Pennington, B. F., Olson, R. K., Chhabildas, N., & Hulslander, J. (2005). Neuropsychological analyses of comorbidity between reading disability and attention deficit hyperactivity disorder: in search of the common deficit. *Dev Neuropsychol, 27*(1), 35-78. doi: 10.1207/s15326942dn2701_3

Worker, A., Blain, C., Jarosz, J., Chaudhuri, K. R., Barker, G. J., Williams, S. C., . . . Simmons, A. (2014). Cortical thickness, surface area and volume measures in Parkinson's disease, multiple system atrophy and progressive supranuclear palsy. *PLoS One, 9*(12), e114167. doi: 10.1371/journal.pone.0114167

Yoshimasu, K., Barbaresi, W. J., Colligan, R. C., Killian, J. M., Voigt, R. G., Weaver, A. L., & Katusic, S. K. (2010). Gender, attention-deficit/hyperactivity disorder, and

reading disability in a population-based birth cohort. *Pediatrics, 126*(4), e788-795. doi: 10.1542/peds.2010-1187

Zhang, Y., Brady, M., & Smith, S. (2001). Segmentation of brain MR images through a hidden Markov random field model and the expectation-maximization algorithm. *IEEE Trans Med Imaging, 20*(1), 45-57. doi: 10.1109/42.906424

Zheng, W., Chee, M. W., & Zagorodnov, V. (2009). Improvement of brain segmentation accuracy by optimizing non-uniformity correction using N3. *Neuroimage, 48*(1), 73-83. doi: 10.1016/j.neuroimage.2009.06.039

ABSTRACT

EVIDENCE OF DISTINCTIVE STRUCTURAL ALTERATIONS THAT DIFFERENTIATE ADHD BOYS WITH AND WITHOUT A COMORBID READING DISABILITY

by

DHRUMAN DILIP GORADIA

August 2015

ADVISOR: Dr. Jeffrey A. Stanley

MAJOR: Translational Neuroscience

DEGREE: Doctor of Philosophy

Attention deficit hyperactivity disorder (ADHD) and reading disability (RD) are neurodevelopmental disorders that often co-occur. Children with ADHD and co-occurring RD (ADHD/+RD) tend to show greater cognitive deficits than children with ADHD alone (ADHD/-RD). However, the extents to which comorbid RD impact structural alteration in children with ADHD have never been investigated. The overall goal of this study was to assess structural alterations in the subcortical, cortical and white matter that may differentiate ADHD/-RD from ADHD/+RD. The general hypothesis was that ADHD/+RD would show extensive alterations in regions implicated in ADHD than ADHD/-RD as well as show additional abnormalities in regions associated with RD.

To this end, structural MRI and DTI scans obtained from 22 ADHD/-RD boys, 15 ADHD/+RD boys and 29 healthy control (HC) boys comparable in age and IQ were analyzed to assess alterations in striatal morphology, cortical thickness and white matter integrity. Analysis of the striatum showed greater and widespread alterations in the caudate in ADHD/+RD relative to ADHD/-RD but not putamen where the alterations were only seen in ADHD/-RD. Similarly, ADHD/+RD showed significantly thinner cortex

in the regions associated with attention and cognitive control as well as additional regions associated with reading relative to ADHD/-RD and HC. However, analysis of DTI parameters showed no significant alterations in white matter structure.

Together, these findings provide evidence of excessive disturbances in the frontostriatal and frontoparietal networks that regulate executive functions, attention and cognitive control. Furthermore, there is evidence of additional alterations in the regions associated with reading skills. Overall, the results indicate a distinctive profile of structural alterations that differentiate ADHD/-RD from ADHD/+RD relative to HC and may underpin the greater neuropsychological impairments observed in ADHD/+RD.

AUTOBIOGRAPHICAL STATEMENT

Dhruman D. Goradia

Education

2015	PhD (Translational Neuroscience Program) Psychiatry and Behavioral Neurosciences Wayne State University School of Medicine, Detroit, MI
2005	MS (Biomedical Engineering) Biomedical, Industrial and Human Factors Engineering Wright State University, Dayton, OH
2001	BE (Instrumentation Engineering) Vidyavardhini's College of Engineering and Technology University of Mumbai, Mumbai, India

Awards and Honors

2013, 2014	Trainee (Educational) Stipend, International Society for Magnetic Resonance in Medicine, Berkeley, CA.
2014	Second prize in poster presentation, Graduate Exhibition, Wayne State University, Detroit, MI.
2012, 2013	Thomas C. Rumble Fellowship, Wayne State University, Detroit, MI.
2013	Summa Cum Laude Merit, Conference Abstract, ISMRM, Salt Lake City, UT.
2013	Second place in poster presentation, GSRD, Wayne State University School of Medicine, Detroit, MI.
2012	Third place in poster presentation, GSRD, Wayne State University School of Medicine, Detroit, MI.

Publications

Goradia DD, Vogel S, Mohl B, Khatib D, Zajac-Benitez C, Rajan U, Robin A, Rosenberg DR, Stanley JA. Altered Surface Morphology of the Striatum in Boys with Attention Deficit Hyperactivity Disorder with and without Comorbid Reading Disability. Biological Psychiatry (In Preparation).

Goradia DD, Frank C, Mohl B, Khatib D, Rajan U, Stanley JA. Evidence Of Pronounced Cortical Thinning In Boys With Comorbid ADHD And Reading Disorder. Biological Psychiatry (In Preparation).

Goradia D, Chugani HT, Munian Govindan R, Behen M, Juhász C, Sood S. Reorganization of the Right Arcuate Fasciculus Following Left Arcuate Fasciculus Resection in Children With Intractable Epilepsy. J Child Neurol. 2011 Oct 1;26(10):1245-50.